Electr Eng (2018) 100:763–785
https://doi.org/10.1007/s00202-017-0547-x

ORIGINAL PAPER

Modeling and control of an interconnected combined cycle gas turbine using fuzzy and ANFIS controllers

Mostafa A. Elhosseini[1] · Ragab A. El Sehiemy[2,5] · Amgad H. Salah[3] · M. A. Abido[4]

Received: 31 August 2016 / Accepted: 29 April 2017 / Published online: 12 May 2017
© Springer-Verlag Berlin Heidelberg 2017

Abstract This paper presents the dynamic modeling of an interconnected two equal area of conventional combined cycle gas turbine. In addition, fuzzy logic controllers have been designed and applied to improve speed/load control, temperature control, and air flow control. The coordination between fuzzy- controlled speed signal and fuzzy-controlled temperature control signal has been considered in the design process using fuzzy fuel controller in order to compute the accurate control signal to the fuel system for fast response against the system disturbance. On the other hand, the adaptive neuro-fuzzy inference system (ANFIS) controller is investigated for controlling the model parameter and selection of the proper rule base in order to improve the proposed controller performance. The results demonstrate the superiority of the proposed model with fuzzy logic controller and ANFIS over the conventional model under normal and abnormal conditions. Moreover, the proposed controllers improve effectively the system damping characteristics after a load deviation as the settling time is greatly reduced.

Keywords Combined cycle gas turbine · Fuzzy logic · Frequency drop · Dynamic response · ANFIS

✉ Ragab A. El Sehiemy
elsehiemy@eng.kfs.edu.eg

[1] Computers Engineering and Control Systems Department, Mansoura University, Mansoura, Egypt

[2] Electrical Engineering Department, Kafrelsheikh University, Kafrelsheikh, Egypt

[3] Electrical Power and Machines Engineering Department, Mansoura University, Mansoura, Egypt

[4] Electrical Engineering Department, King Fahd University of Petroleum and Minerals, Dhahran, Saudi Arabia

[5] Intelligent Systems Research Group (ISRG), Kafrelsheikh University, Kafrelsheikh, Egypt

1 Introduction

Continuous monitoring of electric power generation systems guarantees safe and reliable operation. The available data from electric power plants supplied to the control systems may also be analyzed to confirm appropriate operation, predict future behavior, and allow developing various technologies that enhance the interconnected generating system performance [1]. During last decades, the continuous development in the dynamic performance of interconnected power systems was observed. As a result of numerous advantages of combined cycle power plant (CCPP), it would become an important alternative technology for power generation. The role played by CCPPs on the power generation market includes frequent start-up/shutdown operations, which must be enhanced by means of innovative strategies. To restore the frequency and the power interchange between different areas to their nominal and scheduled values, supplementary control schemes are required to solve the mismatch between the generated and load powers due to unpredictable load variations [2].

Most researchers focused on the automatic generation control (AGC) of the interconnected power systems with many adaptive control techniques [3,4]. The aim of the adaptive controller in AGC was to control the frequency of power systems and inter-area tie line power flow to minimize the area control error (ACE), improve the speed response during disturbance with minimum settling time, and ensure the stability for the power system [5].

In [6], an approach based on genetic algorithm (GA) was suggested for optimizing the AGC parameters of an interconnected power system. To provide more realistic model for AGC design of an interconnected model, the proposed model in [7] considered the generation rate constrains (GRC), dead band, and time delay imposed to power system governor.

For optimal performance of three interconnected reheated systems, integral gains and proportional–integral–derivative (PID) gains were computed [8] by using genetic algorithms. The superiority of PID controller compared to integral controller was reported in [9]. Craziness- based particle swarm optimization presented in [10] proved to be moderately fast algorithm with true optimal gains for AGC of an interconnected two-area power system. In [11], a novel heuristic stochastic search technique has been proposed for optimization of PID gains used in Sugeno fuzzy logic control-based AGC of multi areas thermal unit. In [12], a robust PID controller for AGC of hydroturbine power systems was proposed for controlling the overshoot and enhancing the stability of system dynamics.

The artificial neural networks can be considered an efficient way to tackle complex and ill-defined problems. The development of artificial neural network (ANN) model was issued for efficient and appropriate monitoring of a microgas turbine [13]. In [14], the use of artificial neural networks in modeling and control of power generation systems and load forecasting was presented. An application of layered neural network controller (ANN) has been presented in [15] to study the behavior of four areas interconnected power system controller. Adding superconducting magnetic energy storage (SMES) to the system in [16] improved the system performance. The authors in [17] have compared the performance of an interconnected of four areas with ANN application against genetic algorithms where the results indicate the superiority of ANN application over genetic algorithm.

The authors [18,19] proposed a novel application of artificial neural network ANN-based ANFIS approach to AGC. The results show the improved performance of ANFIS controller in comparison with the conventional integral controller. In [20], the fuzzy logic controller with Gaussian membership function was proposed to study AGC of four area interconnected power system. Demiroren and Yesil [21] investigated the performance of fuzzy logic control for AGC of an interconnected power system including SMES.

Combined cycle gas turbine (CCGT) plays an important role for maintaining standards of security and quality of supply due to its great effect on the frequency regulation of power system. The CCGT has many powerful features that include high energy efficiency, low installation cost, flexibility to fluctuations in electrical load, low maintenance cost, quicker reaction time, and low emission compared to other conventional thermal units [22–24]. The authors in [25] presented a method to transform a combined cycle power plants (CCPP) physical model designed for simulation in an optimization-oriented model to improve start-up performances.

Sasaki and Enomoto [26] focused on studying the dynamic analysis of the system frequency response including the effects of primary and secondary frequency control under normal operation. In [27], the dynamic behavior of a CCPP in the presence of a frequency drop depending on the chain trip-out occurred in Malaysia was investigated. In [28], the variation of CCGT parameters with temperature control was addressed. The dynamic-characteristics analysis of an independent microgrid consisting of a solid oxide fuel cell (SOFC) triple combined cycle TCC and large-scale photovoltaic was discussed in [29].

A comparative analysis for the performance of different types of controller has been discussed in [30], and it is found that PID controller with optimized gains using firefly algorithm gave better performance over integral (I), proportional–integral (PI). A nonlinear model has been introduced in [31,32] for studying the primary frequency regulation of CCGT with parameters identified by genetic algorithm.

Robust controller has been designed for combined cycle power plant gas turbine in [33] to maintain the speed and exhaust temperature within limits by controlling fuel signal and compressor inlet guide vane (IGV) position. Simulation results show the improvement in the performance compared to PID control.

A fuzzy logic controller was designed to stand-alone hybrid power generation system of wind turbine, microturbine, solar array, and battery storage to satisfy the load demand under all conditions for extraction of maximum energy from a variable speed wind power generation system [34].

In [35], a fuzzy logic controller was implemented for the governing system. The results obtained during start-up and picking load operation showed better results with the PID control and robust controller. However, the dynamic response of CCGT due to frequency change has not been investigated.

In [36], the authors focused on the implementation of fuzzy logic control and the combination between fuzzy logic control and proportional control to obtain the required speed response of CCGT under normal and transient operation conditions. The performance of CCGT has been developed in [37] by designing a fuzzy logic controller on blade path temperature to activate the high- temperature runback control. A fuzzy logic controller was also designed for the throttle pressure limits, which compute the better value of the bypass valve demand to get the steam turbine demand. However, the response time of steam turbine was large and the valve position dynamic for gas turbine was oscillatory.

To conclude the previous work, most of the literature for AGC implemented conventional integral (I), proportional–integral (PI), and proportional–integral–derivative (PID) controllers with fixed structure and constant parameters tuned at one operating condition. Since the characteristics of the power system elements are continuously changing, these controllers may not be capable of providing the desired performance at different operating conditions due to lack of robustness. Several intelligent techniques such as fuzzy

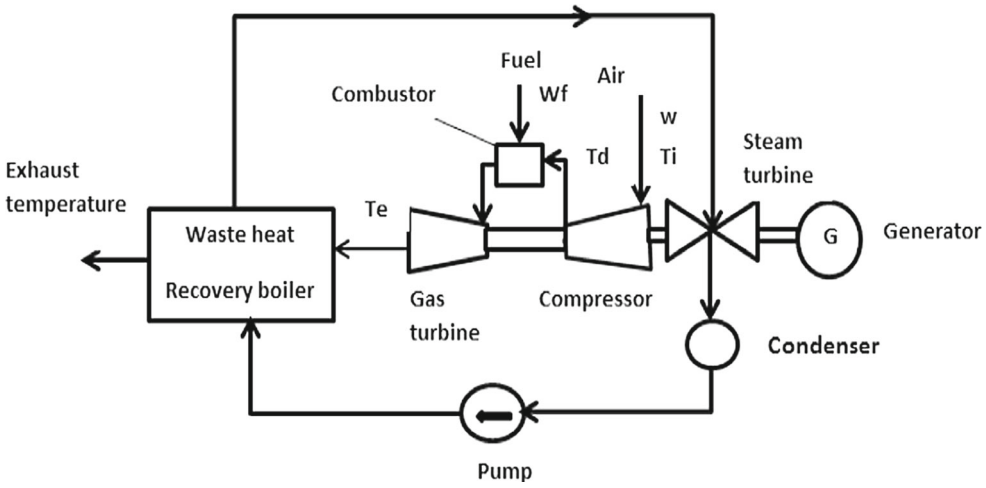

Fig. 1 Single-shaft combined cycle gas turbine

logic control (FLC), artificial neural network (ANN), ANFIS, genetic algorithm (GA), and bacteria foraging (BF) are used extensively in the isolated as well as interconnected power systems [38].

In this paper, the fuzzy logic and ANFIS controllers are proposed to enhance the dynamic response of a two-area interconnected CCGT power system due to their flexibility in decision-making process. The proposed controllers provide an efficient way to cope with imperfect information and avail an interesting human machine interface by simplifying rule extraction from human experts. The proposed fuzzy logic controllers use triangular membership functions to control speed/load, temperature limit, and air flow. In addition, the coordination between fuzzy-controlled speed signal and fuzzy- controlled temperature control signal has been considered in the design process. On the other hand, a sincere attempt is made to reduce the response settling time by proposing an efficient controller using ANFIS control strategy. The adaptive network employs an optimization algorithm to tune parameters of fuzzy inference system. Improving the dynamic response of the interconnected CCGT power system employed under normal operation and restoring the frequency and power transfer via the tie line under load variations.

The rest of this paper is organized as follows: Sect. 2 covers the problem formulation, while the proposed controller design of fuzzy logic controller is presented in Sect. 3. ANFIS controller is covered in Sect. 4. Finally, simulation results and discussions are presented in Sect. 5.

2 Proplem formulation

Figure 1 shows the single-shaft combined cycle gas turbine. The plant consists of compressor, combustor, gas turbine, waste heat recovery boiler, steam turbine, and generators. It combines two thermodynamic cycles. In gas turbine, the air is provided to the compressor which compresses the air and draws it into combustion chamber. The compressed air is mixed with the fuel, and the mixture is ignited to make high-temperature gases that drive to gas turbine. The high exhaust gases are recovered steam generator (HRSG) that provides the steam turbine by the required proper steam [39–42]. The chain of sub models of combined cycle gas turbine described above is shown in Fig. 2. The details of each of these sub models are developed in the next section. The plant power output is the sum of the gas turbine and steam turbine outputs. The mathematical equations of the dynamic parts of CCGT are derived blow [43,44].

The airflow in gas turbine (W) is compressed adiabatically so the compressor discharge temperature T_{d} can be calculated as follows:

$$W = W_{\mathrm{a}} \frac{P_{\mathrm{a}}}{P_{\mathrm{a0}}} \frac{T_i}{T_{i0}}, \tag{1}$$

$$X = (P_{\mathrm{ro}} W)^{\alpha - 1/\alpha}, \tag{2}$$

$$T_{\mathrm{d}} = T_{\mathrm{i}} \left(1 + \frac{x-1}{n_{\mathrm{c}}}\right), \tag{3}$$

where P_{ao} is rated atmospheric pressure, $T_{\mathrm{io}}(k)$ rated atmospheric temperature, W_{a} airflow at P_{ao} and T_{io} (assume $P_{\mathrm{ao}} = P_{\mathrm{a}}$), W airflow in per unit of its rated value, and P_{a} atmospheric pressure.

Gas turbine inlet temperature T_{f} is calculated from the combustor heat balance:

$$T_{\mathrm{f}} = T_{\mathrm{d}} + (T_{\mathrm{fo}} - T_{\mathrm{do}}) \frac{W_{\mathrm{f}}}{W}, \tag{4}$$

where W_{f} is the fuel flow in per unit of its rated value

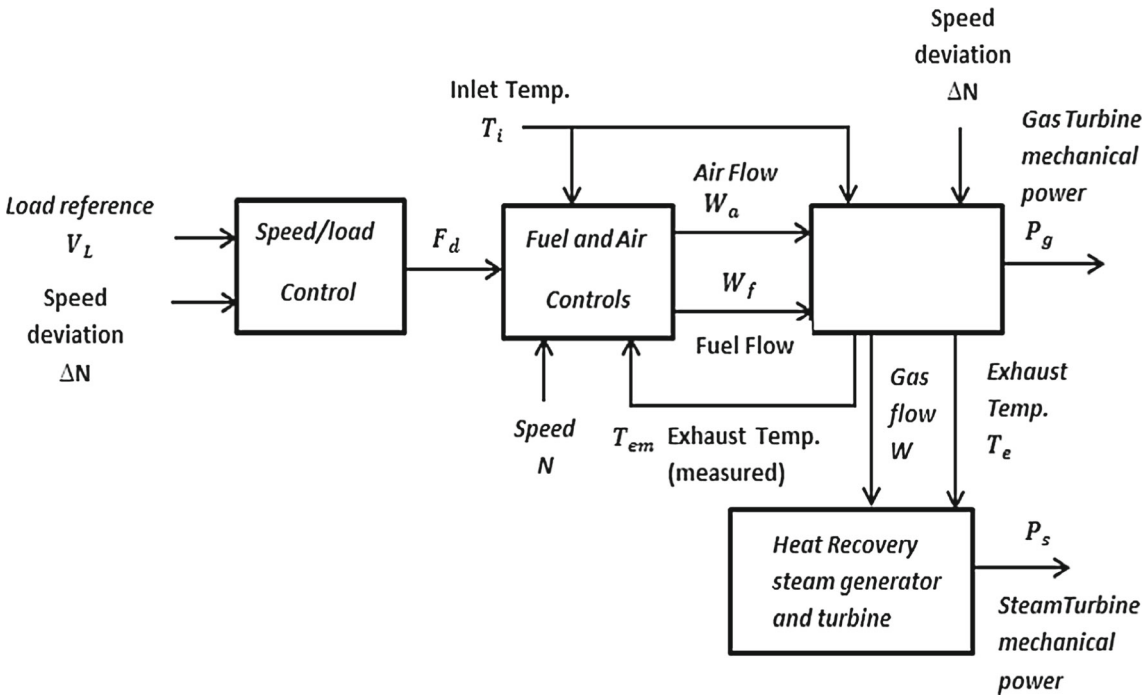

Fig. 2 Sub model of combined cycle gas turbine

The fuel flow is a negligible amount compared to the airflow. Gas turbine exhaust temperature T_e is described as follows:

$$T_e = T_f \left[1 - \left(1 - \frac{1}{x}\right) n_t\right], \tag{5}$$

The exhaust gas flow is practically equal to the airflow. Moreover, the net energy provided to the gas turbine (E_g) for both areas can be calculated as follows:

$$E_g = K_o \{(T_f - T_e) - (T_d - T_i)\} W, \tag{6}$$

Steam turbine and heat recovery boiler depend on the exhaust gases out from gas turbine, which collects some energy (E_s) that can be calculated as follows:

$$E_s = K_1 T_e W, \tag{7}$$

Area 1 and area 2 contain combined cycle gas turbine as shown in Fig. 3. The turbine reference power of each area is set by an integral controller. The frequencies of each area are affected by each other and also the tie line power variation. The summation of frequency variation and tie power variation which is called area control error (ACE) is the input of the integrator as follows.

$$\boldsymbol{ACE_1} = \Delta \boldsymbol{p_{12}} + \boldsymbol{B_1} \Delta \boldsymbol{f_1} \tag{8}$$

$$\boldsymbol{ACE_2} = \Delta \boldsymbol{p_{21}} + \boldsymbol{B_2} \Delta \boldsymbol{f_2} \tag{9}$$

where B_1 and B_2 are the frequency biasing factors of areas 1 and 2, respectively.

The model consists of several blocks that describe the control circuits such as speed/load control, temperature control, fuel control, air control and other blocks for gas turbine, wasted heat recovery boiler/steam turbine, rotor shaft, and temperature transducer [45–47]. The model described in this paper is not intended for use for simulation of start-up, shutdown operation so that an acceleration control is generally neglected in this model.

- The speed/load block (governor) is activated when there is any speed deviation from the nominal value. It sends a control signal participating with exhaust temperature control signal to low value selector, which determines the required fuel signal control. Descriptions of parameters are provided in "Appendix"
- The temperature control block contributes to speed/load control signal in determining fuel control signal for the fuel system. The measured exhaust temperature is compared with the reference exhaust temperature. d the error acts on temperature control. To keep thermodynamic limits of the unit, the measured exhaust temperature must not exceed the reference temperature.
- Air flow control is based on the exhaust temperature. It adjusts the required air flow through control the inlet guide vans position to keep the exhaust temperature under limits and preserve thermodynamic limits of the unit.

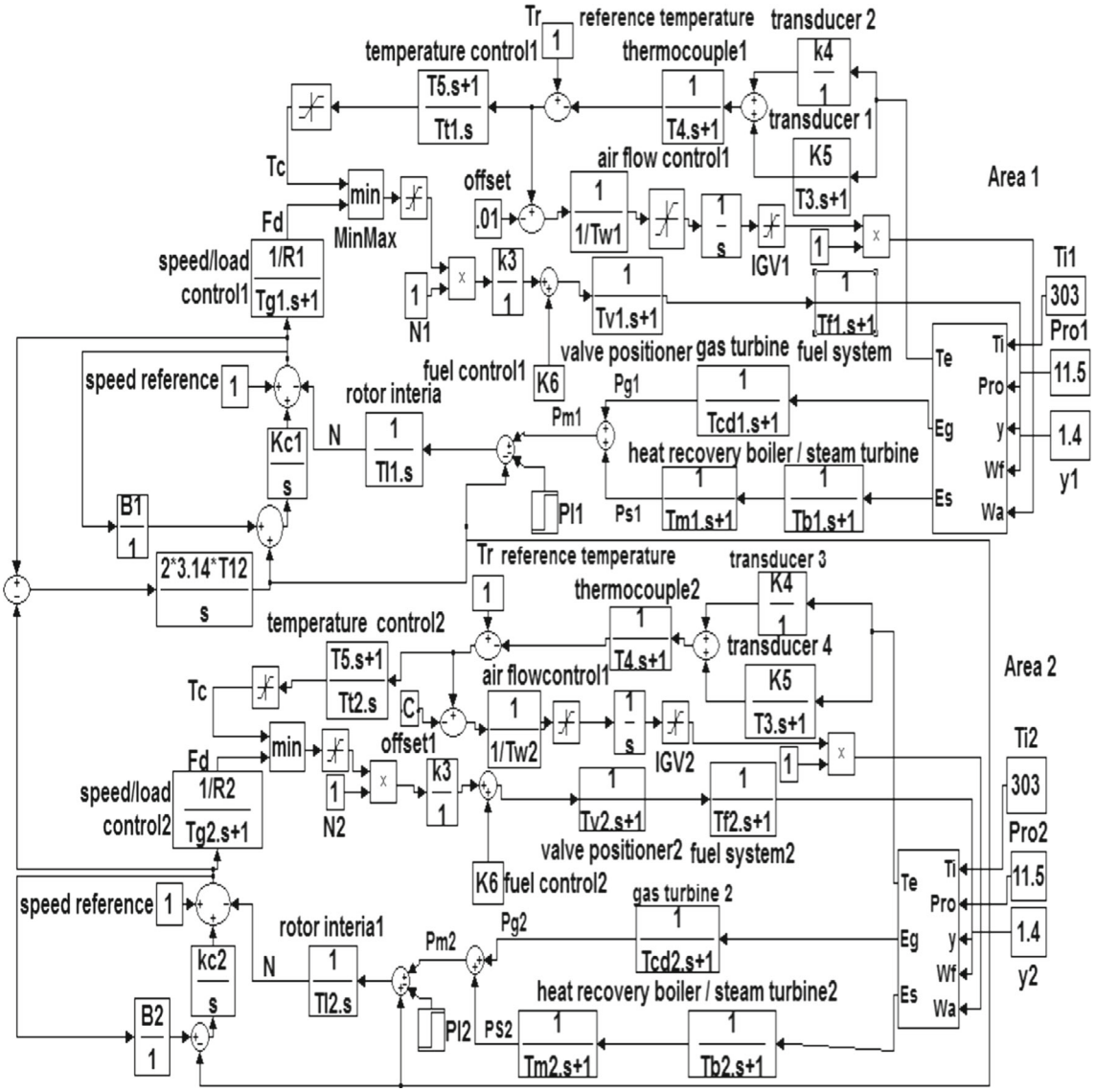

Fig. 3 Simulink model of two equal areas of combined cycle gas turbine

- Fuel control system depends on the output signals from the speed/load block and the temperature control block. A low value selector compares these signals and selects the lower one to determine the required amount of fuel flow.

3 Proposed fuzzy logic controller design

Fuzzy logic controller is introduced by Zadeh [48] where human experts and process knowledge are used to create the control rules. The most widely used type of Mamdani is used in this study since it is easy to design and implement. The main components of fuzzy logic controller used in this work are:

- Rule base—it contains expert's knowledge, as a set of rules, and process knowledge about how to control the system.
- Fuzzification interface—it converts the fuzzy inputs in order to interact with the rule based.
- Inference mechanism—it selects the control rules that are effective and decide the control signal that must be generated.
- Defuzzification interface—it converts the fuzzy value to crisp value which this value is usually required to control process system.

In this study, four fuzzy logic controllers for speed/load control, temperature control, air flow control, and fuel flow control have been considered for each areas of the intercon-

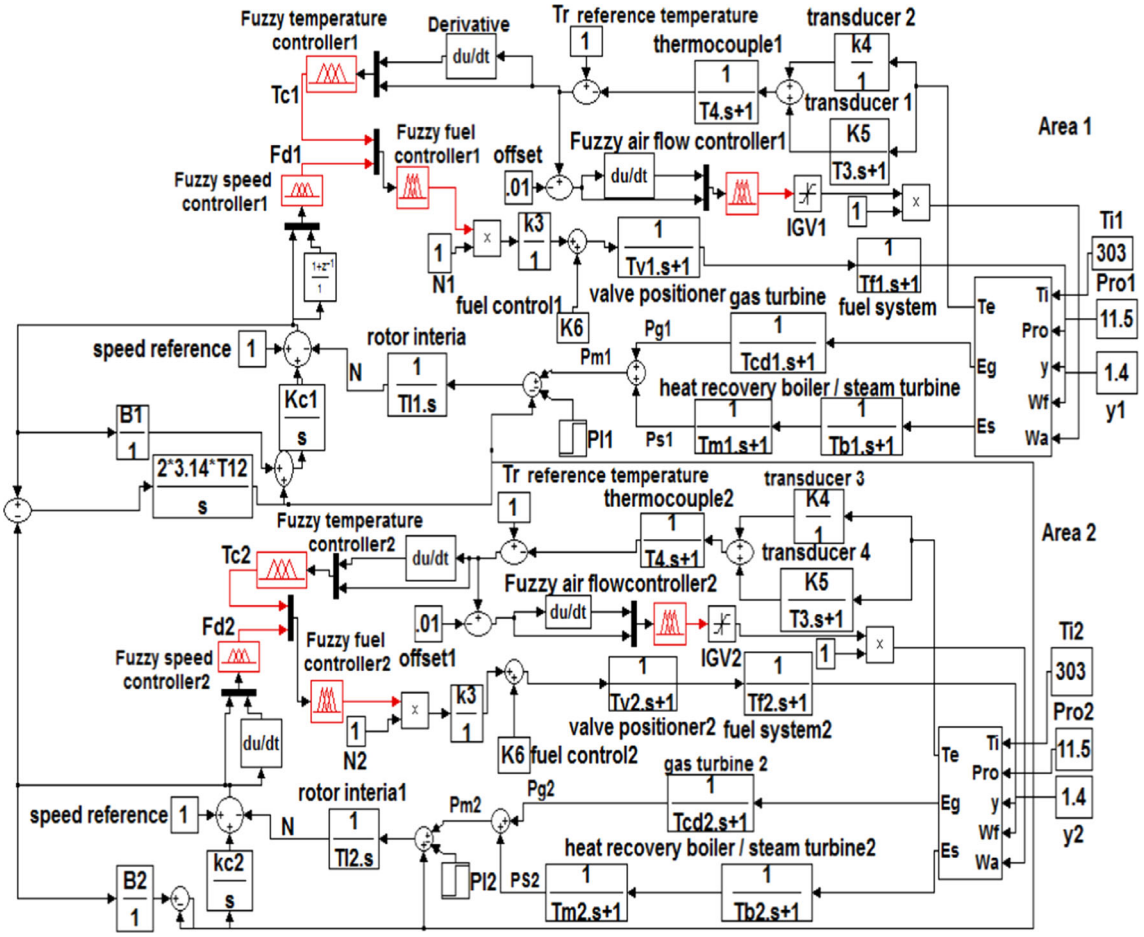

Fig. 4 Simulink model of two equal areas of combined cycle gas turbine with fuzzy logic controller

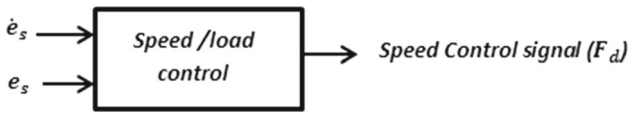

Fig. 5 Fuzzy speed/load control

nected system as shown in Fig. 4. Detailed descriptions of the proposed controllers are given below.

3.1 Fuzzy speed/load controller

The proposed fuzzy speed/load controller is used instead of classical speed governor as shown in Fig. 4. The inputs to the proposed fuzzy speed/load controller are the speed/load error (e_s) and the rate of change of speed/load error ($\dot{e}_s$), and the output is the speed control signal (F_d) as shown in Fig. 5. The inputs have five membership function of triangular type as well as the output as shown in Fig. 6. The range of each membership is selected by executing numerous experiments to identify it. The inference operation is made according to the inference given in Table 1.

3.2 Fuzzy temperature control system

To improve the dynamic response of CCGT, a proposed fuzzy temperature control system is used instead of overheating control system as shown in Fig. 4. In Fig. 7, the inputs to the fuzzy temperature control are the temperature error (e_t) between the measured exhaust temperature and the reference exhaust temperature (T_r) and temperature error rate ($\dot{e}_t$). The output is the temperature control signal (T_c) that contributes the speed/load control signal (F_d) to determine an accurate required amount of fuel. The inputs have five membership specific functions of triangular type as well as the output as shown in Fig. 8 where the ranges of membership functions are selected through executing numerous experiments. Linguistic rules are similar to that of Table 1.

3.3 Fuzzy air flow control system

Fuzzy air flow control system is proposed to improve the dynamic response of the air flow system. Figure 9 shows the inputs to the fuzzy air flow control which are the temperature

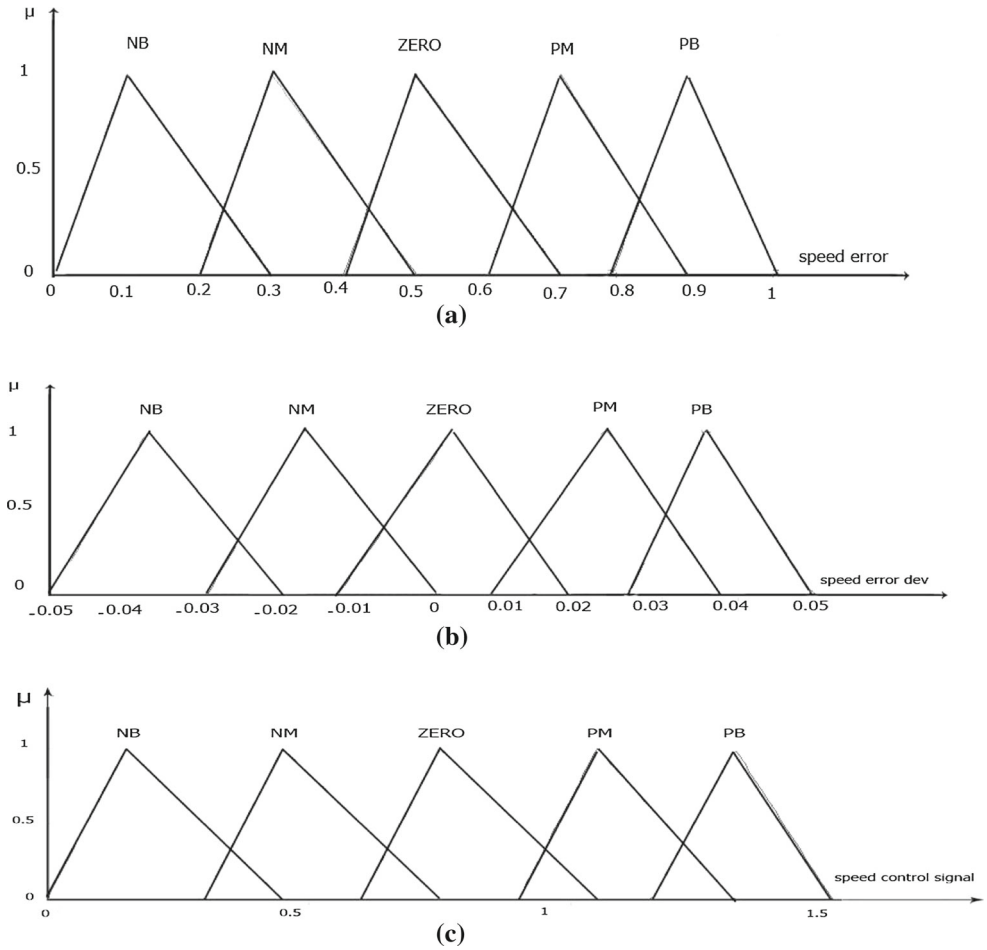

Fig. 6 Fuzzy speed/load control system membership function. **a** Membership function of speed error input. **b** Membership function of speed error deviation input. **c** Membership of speed control signal output

Table 1 Linguistic values of the proposed fuzzy logic controllers

$e/\dot{e}$	NB	NM	ZE	PM	PB
NB	NB	NB	NB	NM	ZE
NM	NB	NB	NM	ZE	PM
ZE	NB	NM	ZE	PM	PB
PM	NM	ZE	PM	PB	PB
PB	ZE	PM	PB	PB	PB

Table 1 includes the 25 linguistic rules of the membership functions where: *NB* negative big, *NM* negative medium, *ZE* zero error, *PM* positive medium, *PB* positive big

error (e_t) between the measured exhaust temperature and the reference exhaust temperature (T_r) and temperature error rate ($\dot{e}_t$) and the output is the air control signal that adjust inlet guide vans (IGV) and limits the required amount of air flow at different operation modes. The inputs have five membership specific functions of triangular type as well as the output as shown in Fig. 10. The inference operation is made according to the linguistic rules given in Table 1.

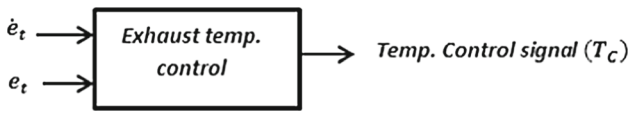

Fig. 7 Fuzzy exhaust temperature control

3.4 Fuzzy fuel control system

The new fuzzy control system is used to optimize the input signal to the fuel system as shown in Fig. 4. It has two inputs speed control signal (F_d) and temperature control signal (T_c), and the output is the control signal to the fuel system as shown in Fig. 11. The inputs have five membership specific functions of triangular type as well as the output as shown in Fig. 12. The linguistic variables of the fuzzy fuel control are shown in Table 2.

Generally, the sequential design of different controllers does not guarantee the optimal performance due to the dynamic interaction among the controllers. In complex systems, some controllers may have adverse effects on the other

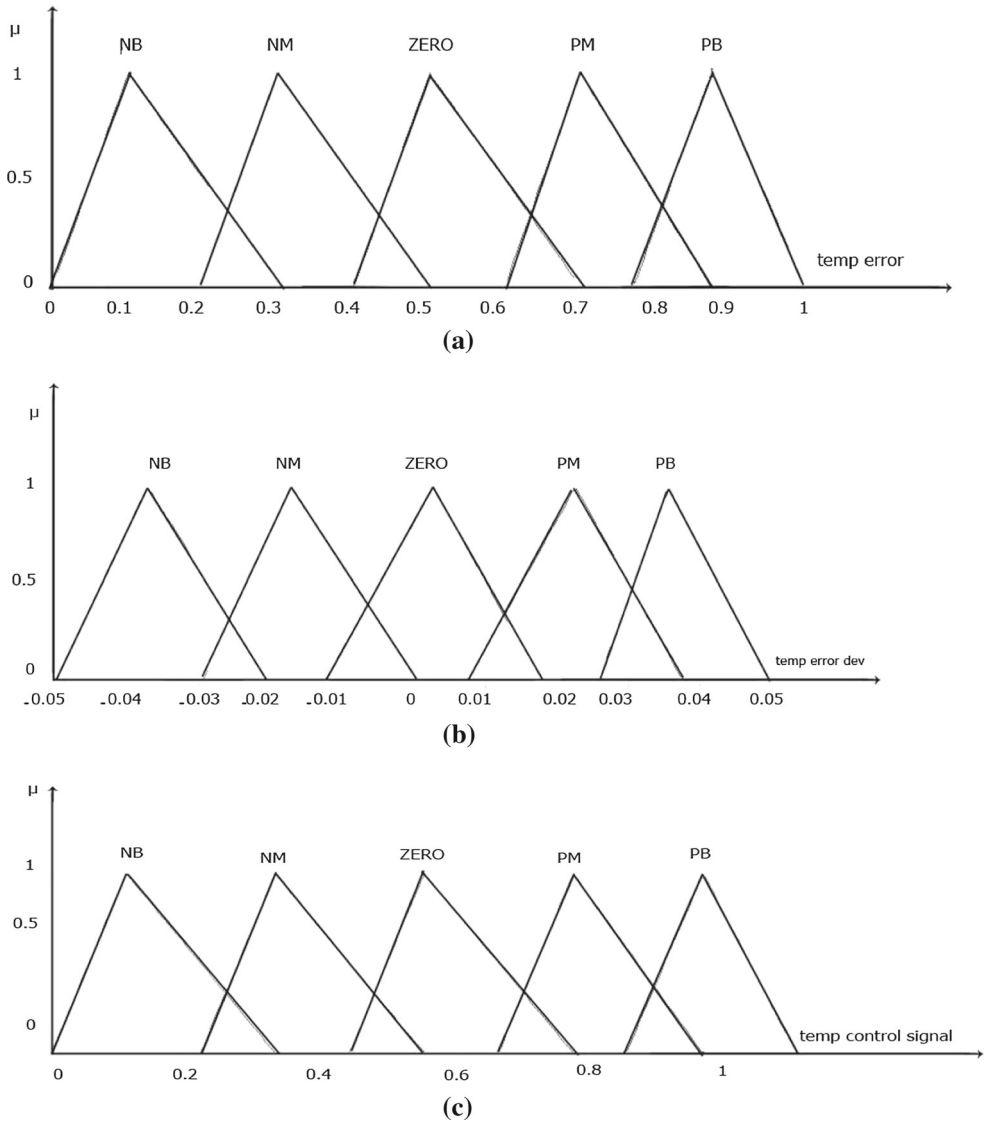

Fig. 8 Fuzzy temperature control system membership functions. **a** Membership function of temperature error input. **b** Membership function of temperature error rate input. **c** Membership function of temperature control signal output

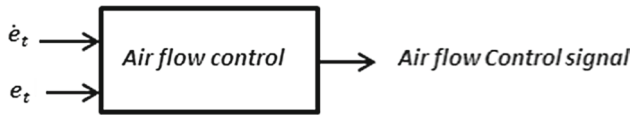

Fig. 9 Fuzzy air flow control

controllers leading to poor performance of the overall system. To avoid such a problem, the proposed controllers in this study have been designed simultaneously to ensure their optimal performance and coordination among them.

4 Adaptive neuro-fuzzy inference system (ANFIS)

ANFIS controller combines the flexibility and subjectivity of fuzzy inference system as well as quick response and adaptability nature of artificial neural network (ANN). The most commonly used fuzzy system in ANFIS architecture is the Sugeno model since it is less computationally exhaustive and more transparent than other models. The adaptive network employs an optimization algorithm to tune parameters of fuzzy inference system. The adaptation process aims to obtain a set of parameters at which an error measured between the actual performances of the fuzzy model and a targeted set of training data is minimized. The typical structure of ANFIS controller is shown in Fig. 13.

Recently, a rapid growth in the number and variety of applications based on ANFIS controller such as industrial manufacturing and automatic generation control is observed. The proposed ANFIS controller is applied to load frequency control of a two equal area of CCGT system connected

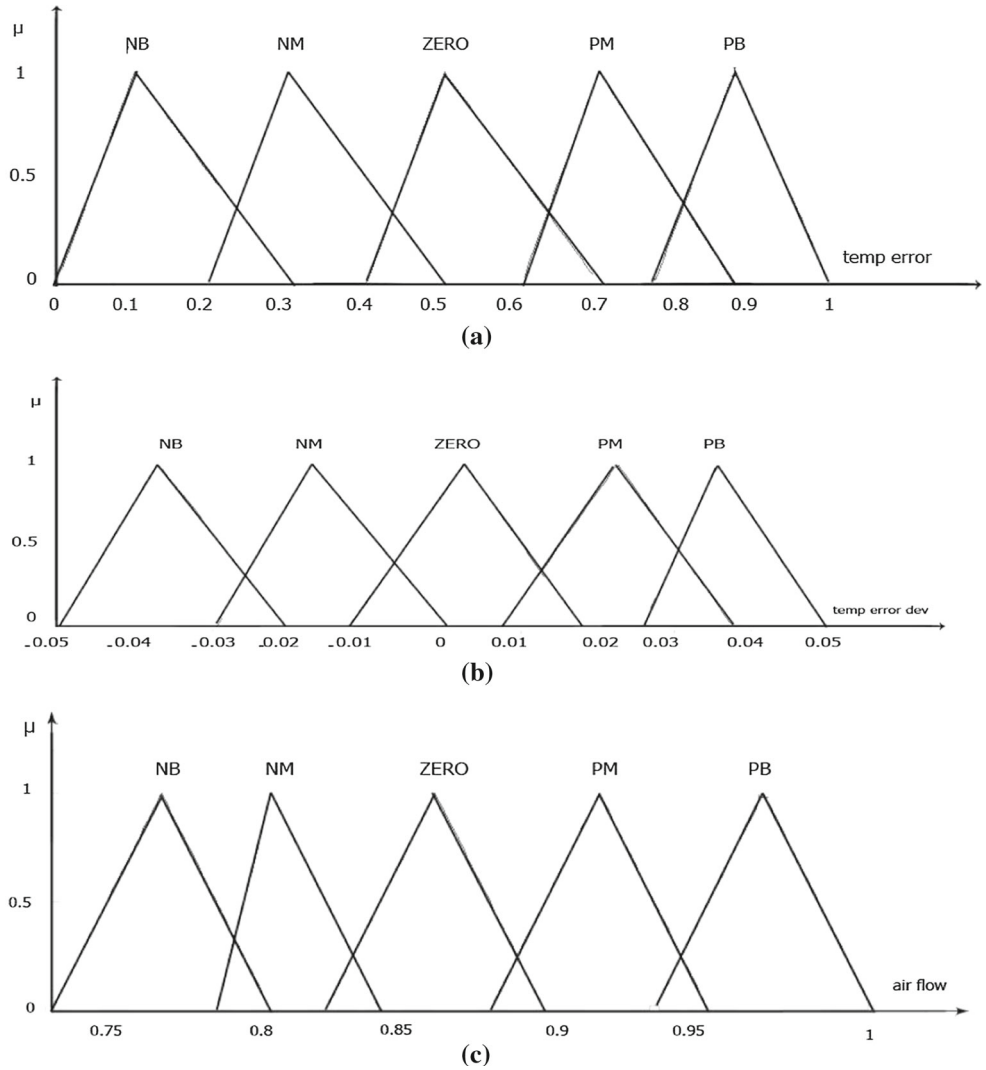

Fig. 10 Fuzzy air flow control system membership functions. **a** Membership function of temperature error input. **b** Membership function of temperature error rate input. **c** Membership function of air flow signal output

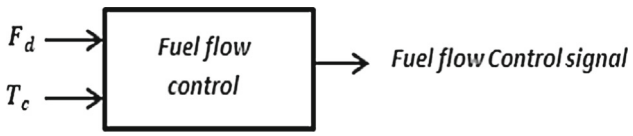

Fig. 11 Fuzzy fuel flow control

through power line to achieve a better dynamic performance. Detailed descriptions of the proposed ANFIS controller for speed/load system and temperature control system are given below.

4.1 Proposed speed/load control with ANFIS

The proposed ANFIS controller is used instead of classical speed governor. The simplified block diagram of the speed/load controller is shown in Fig. 14. It has two input signals. These are the error of speed/load signal and the rate of error signal. The membership functions of input variables, linguistic variables, and value ranges are given in Fig. 15.

4.2 Proposed temperature control with ANFIS

The simplified block diagram of the proposed temperature controller with ANFIS is shown in Fig. 16. The inputs to the proposed temperature controller are the temperature error between the measured exhaust temperature and the reference temperature, and the second input is the rate of temperature error signal. The membership function of input variables of temperature controller with ANFIS, linguistic variables, and value ranges are given in Fig. 17.

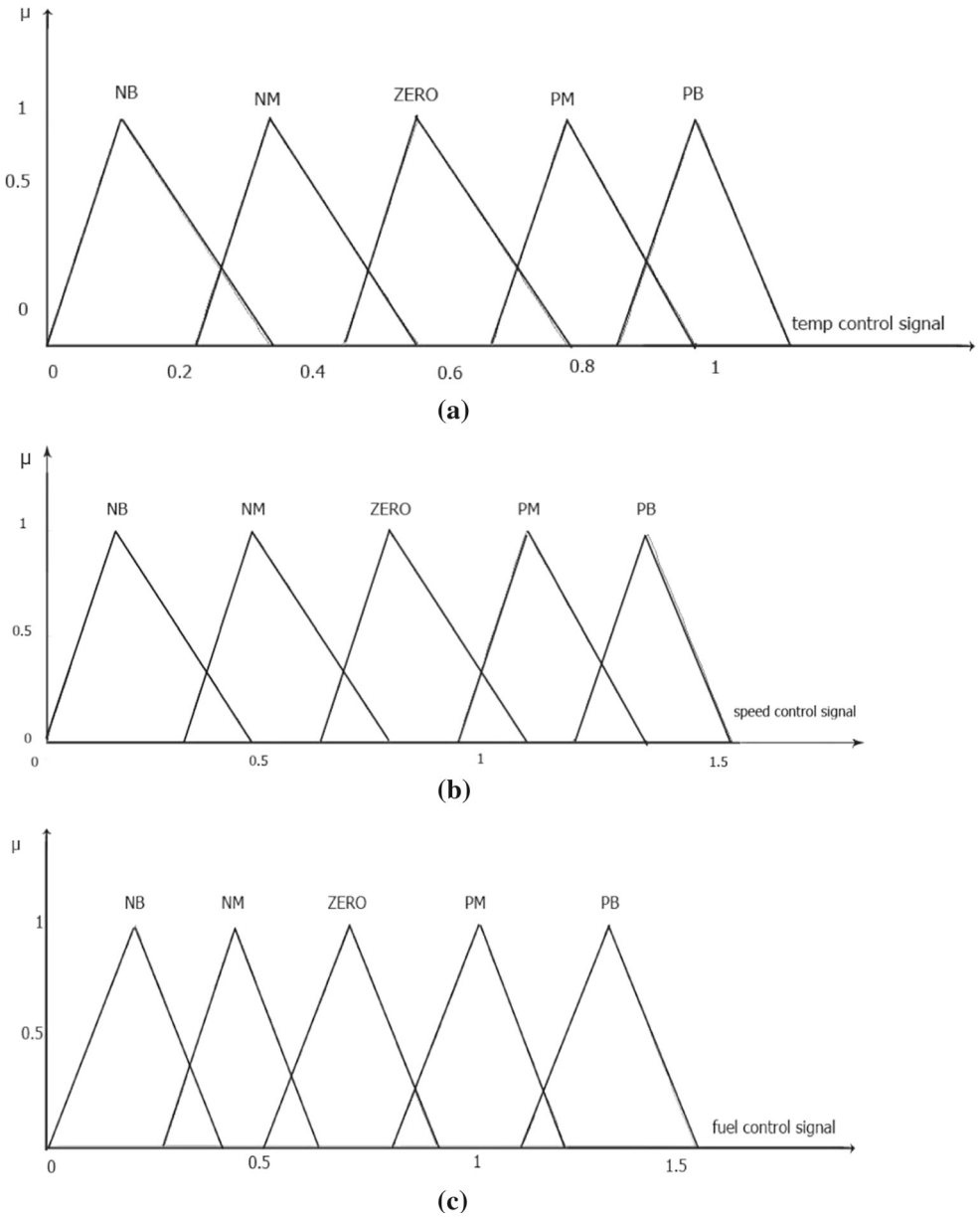

Fig. 12 Fuzzy fuel control system membership functions. **a** Membership function of temperature control signal input. **b** Membership of speed control signal input. **c** Membership of fuel control signal input

Table 2 Linguistic values of the membership function of the fuel control input and output

F_d/T_C	NB	NM	ZE	PM	PB
NB	NB	NB	NB	NB	NB
NM	NB	NM	NM	NM	NM
ZE	NB	NM	ZE	ZE	ZE
PM	NB	NM	ZE	PM	PM
PB	NB	NM	ZE	PM	PB

5 Simulation results and discussions

5.1 Choice and selection of membership function

There are many potential types of membership function shapes for the fuzzy logic inputs and outputs. Among all membership functions, triangular membership function and trapezoidal membership function were chosen as they are the most common and easy to implement. In this study, the opti-

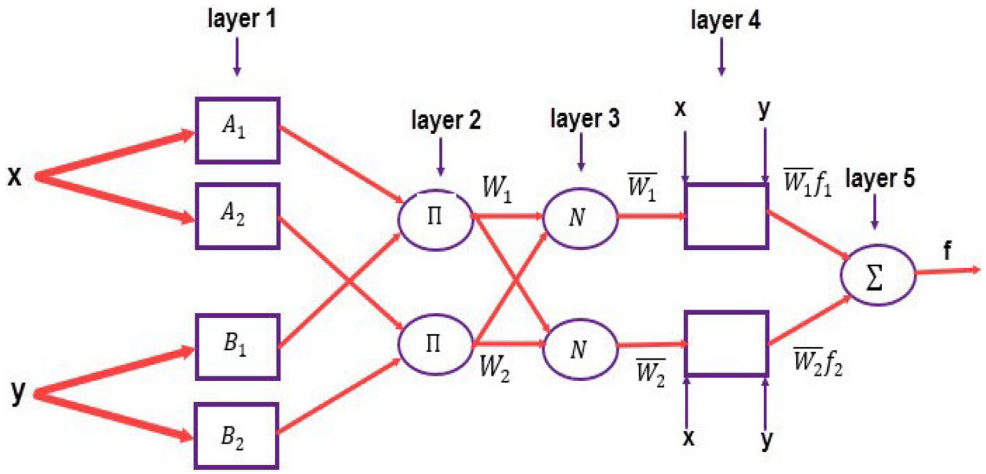

Fig. 13 A general schematic diagram of ANFIS controller system

Fig. 14 Simulation block diagram of speed/load control with ANFIS

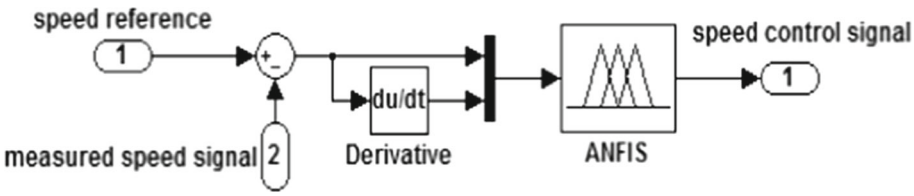

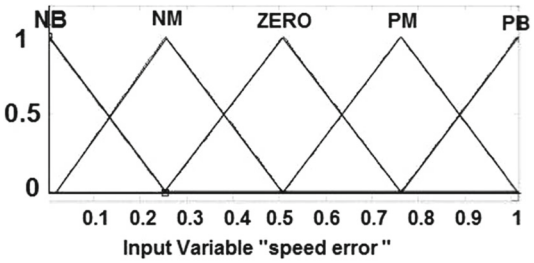

(a)

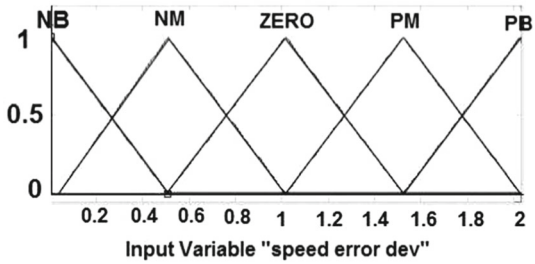

(b)

Fig. 15 Membership functions of speed/load control with ANFIS. **a** Membership functions of speed error input variable of ANFIS. **b** Membership functions of speed error deviation input variable of ANFIS

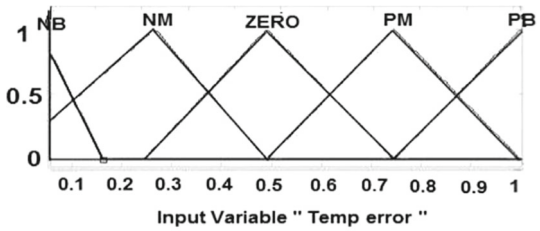

(a)

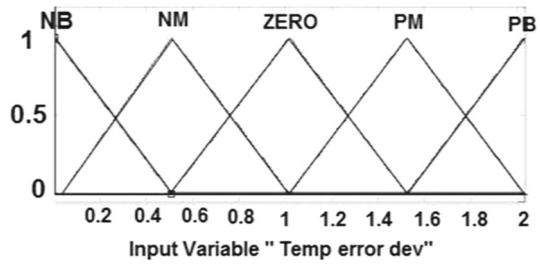

(b)

Fig. 17 Membership functions of temperature control with ANFIS. **a** Membership functions of temperature error input variable of ANFIS. **b** Membership functions of temperature error deviation input variable of ANFIS

Fig. 16 Simulation block diagram of temperature control with ANFIS

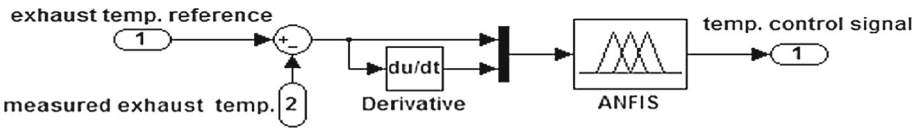

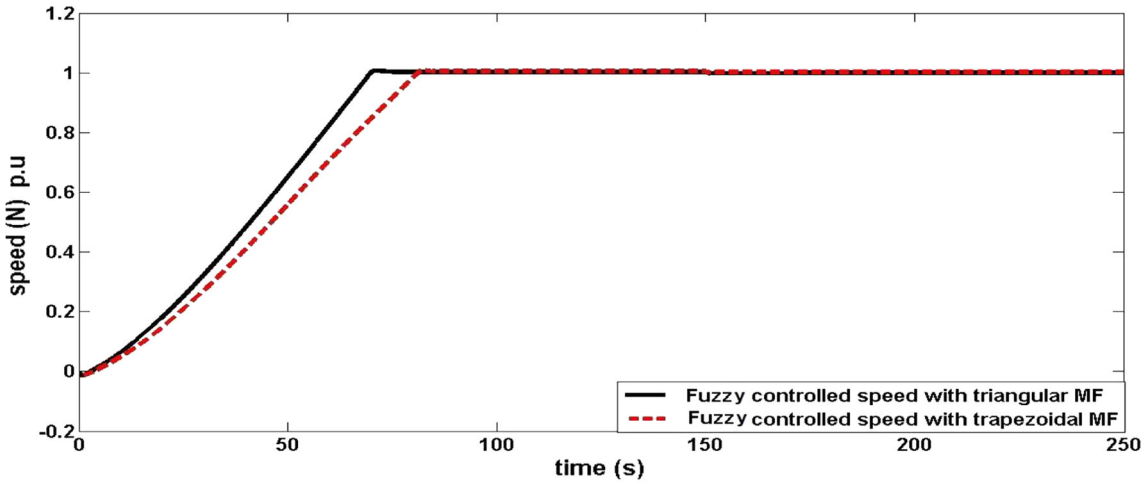

(a)

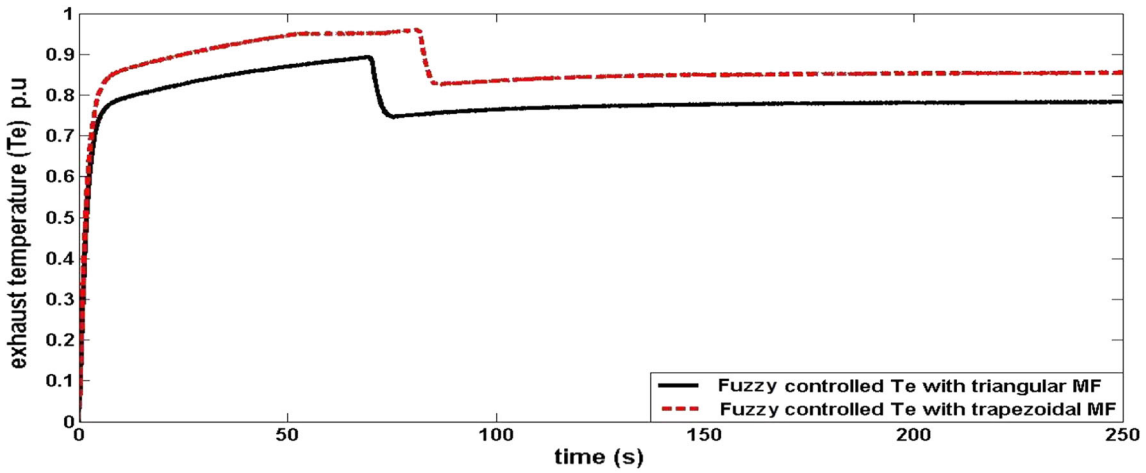

(b)

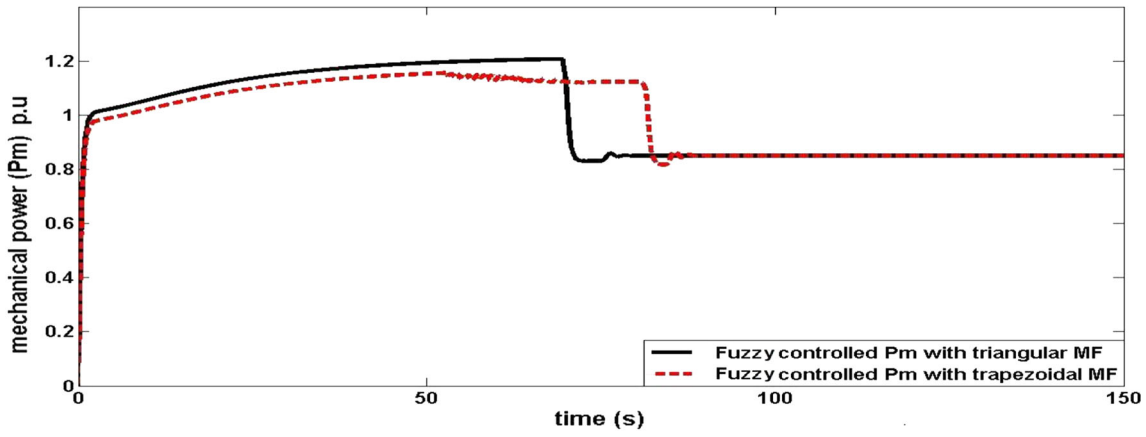

(c)

Fig. 18 Dynamic response of a two area of CCGT with fuzzy logic controller for both triangular and trapezoidal mf. **a** Speed (N) of CCGT. **b** Exhaust temperature (T_e) of CCGT. **c** Mechanical power (P_m) of CCGT

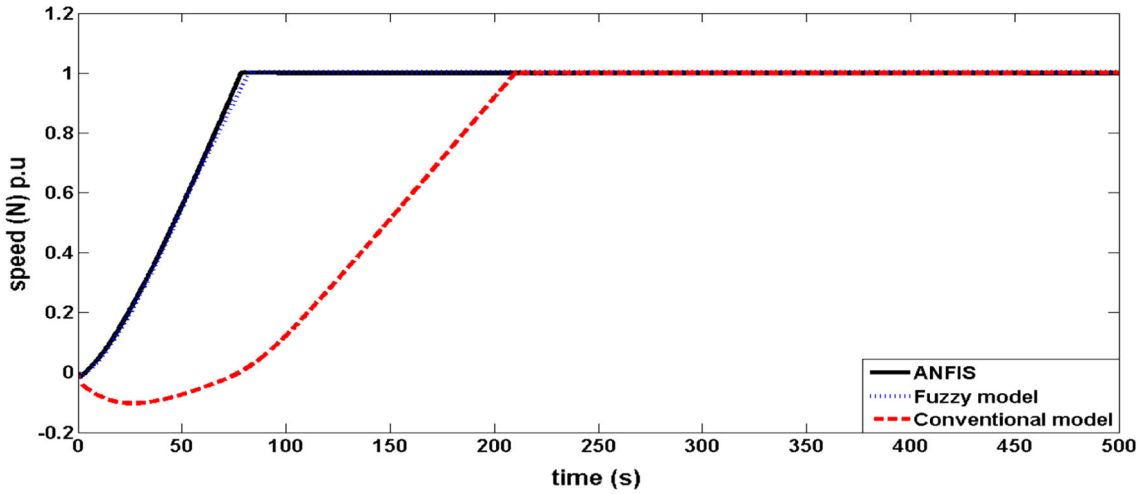

(a)

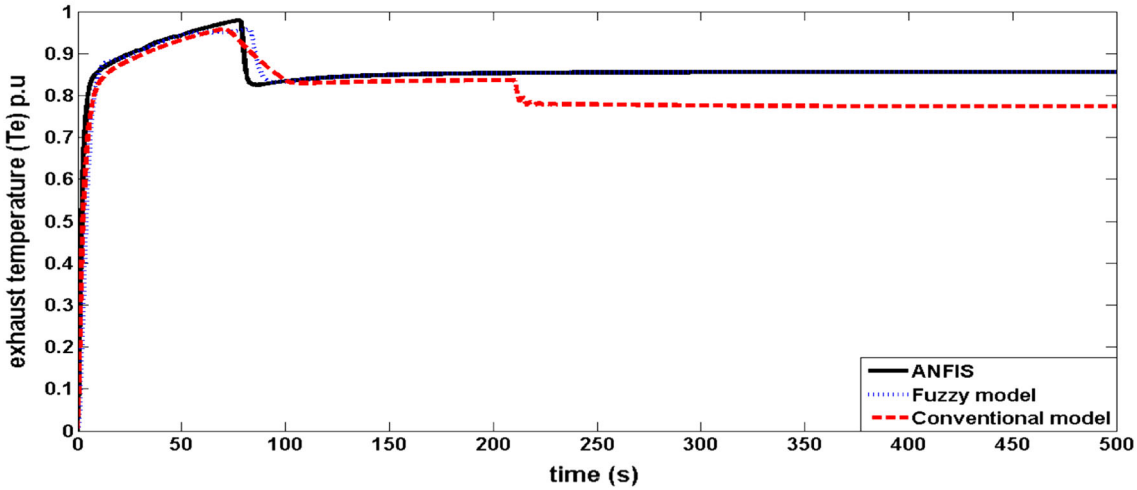

(b)

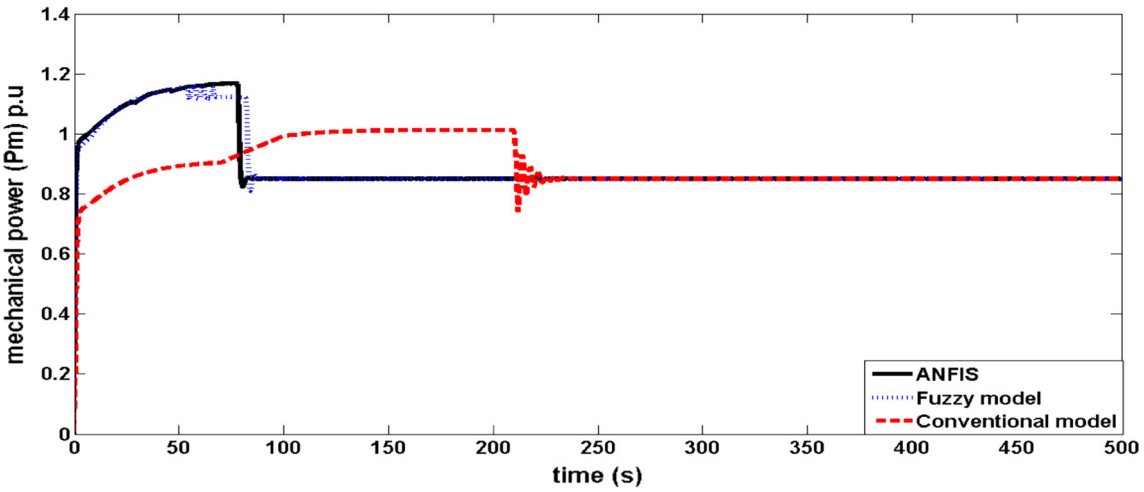

(c)

Fig. 19 Dynamic response of a two area of CCGT with fuzzy logic controller and conventional control under normal operation. **a** Speed (N) of CCGT. **b** Exhaust temperature (T_e). **c** Mechanical power (P_m). **d** Air flow (Wa) of CCGT

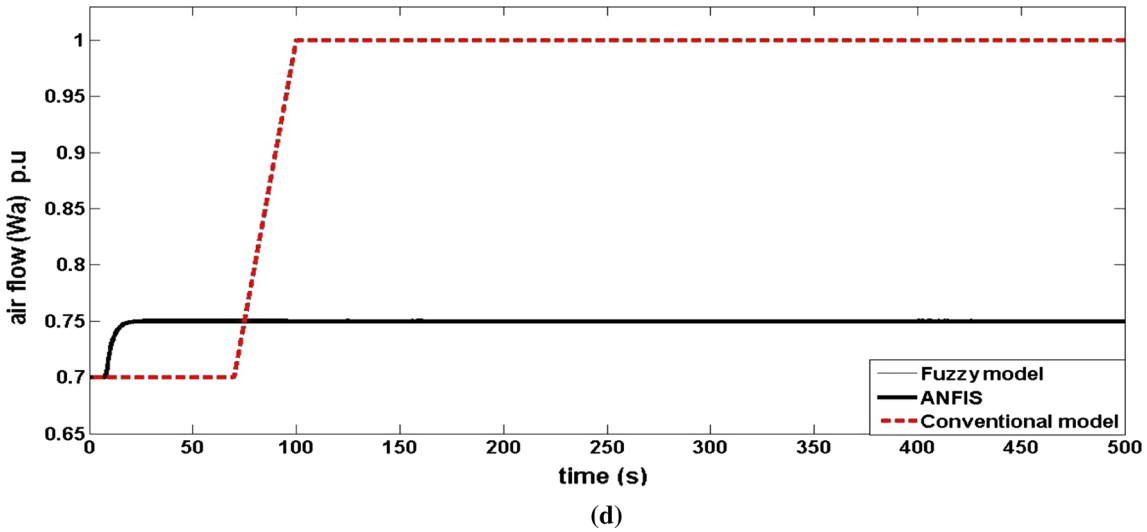

(d)

Fig. 19 continued

mal shape of the membership functions is selected by testing the fuzzy controllers with each shape of membership functions under normal operation condition. The results indicate that triangular membership function gives better results than trapezoidal membership functions as shown in Fig. 18.

The proposed model of two equal interconnected area of combined cycle gas turbine including the proposed fuzzy logic and ANFIS controllers has been tested and compared to the conventional controllers. The dynamic response of the two models has been evaluated under normal operation and load perturbation conditions. The load perturbation is simulated by changing the demand from 0.85 to 1 p.u and from 0.85 to 0.7 p.u.

5.2 Response under normal operation

The simulation results at normal operation ($P_L = .85$) are presented in Fig. 19. It is observed that the speed response for both fuzzy logic controller and ANFIS controller is approximately similar. Furthermore, it is clear that the speed response for both fuzzy logic and ANFIS controllers is much better than that of the conventional controllers as the settling time has been reduced from 198.4576s with conventional controllers to 74.9663s only with the proposed controller of fuzzy logic controller, while in ANFIS is 73.6166s as shown in Table 3. Figure 19b shows clearly that the exhaust temperature response of the proposed ANFIS and fuzzy logic controllers is almost similar. In addition, both controllers achieve better dynamic performance compared to conventional ones as shown in Table 4. It can be seen that the exhaust temperature for both fuzzy logic and ANFIS controllers reaches to maximum exhaust gas temperature (0.85 p.u); however, the exhaust temperature of conventional model needs more time to reach to its maximum value (0.78).

Table 3 Speed response of an interconnected CCGT system

Comparative coefficients	Conventional model	Fuzzy model	ANFIS
Rise time	94.1984	53.6591	51.6214
Settling time	198.4576	74.9663	73.6166
Overshoot	0.4132	0.4319	0.2554
Peak time	201.9898	77.3265	75.3106

Table 4 Temperature response of an interconnected ccgt system

Comparative coefficients	Conventional model	Fuzzy model	ANFIS
Rise time	8.5186	6.1223	3.7558
Settling time	207.9578	110.8823	109.4405
Overshoot	22.9328	11.8144	14.4354
Peak time	70.4723	81.2071	74.9263

Table 5 Mechanical power response of an interconnected CCGT system

Comparative coefficients	Conventional model	Fuzzy model	ANFIS
Rise time	6.8508	0.6211	0.62
Settling time	211.6532	84.8976	81.1345
Overshoot	19.1780	36.6772	37.3530
Peak time	200.5894	61.930	71.515

The response of the mechanical power of the interconnected model with ANFIS controller, fuzzy logic controller and conventional controller is shown in Fig. 19c. As seen from the figure, similar result was obtained for both fuzzy logic controller and ANFIS controller where the superiority

Table 6 Air flow response of an interconnected CCGT system

Comparative coefficient	Conventional model	Fuzzy model	ANFIS
Rise time	24	6.5911	6.5911
Settling time	99.4	19.8604	19.8604
Peak	1	0.75	0.75
Peak time	100	25	25

of fuzzy logic control and ANFIS controller is evident. The comparison between the responses based on the time domain specifications is shown in Table 5. It can be seen from Fig. 19d that the inlet guide vanes start opening to allow more flow of air and thus reducing the exhaust temperature. From Table 6, it may be noted the effectiveness of the proposed model compared to the conventional model.

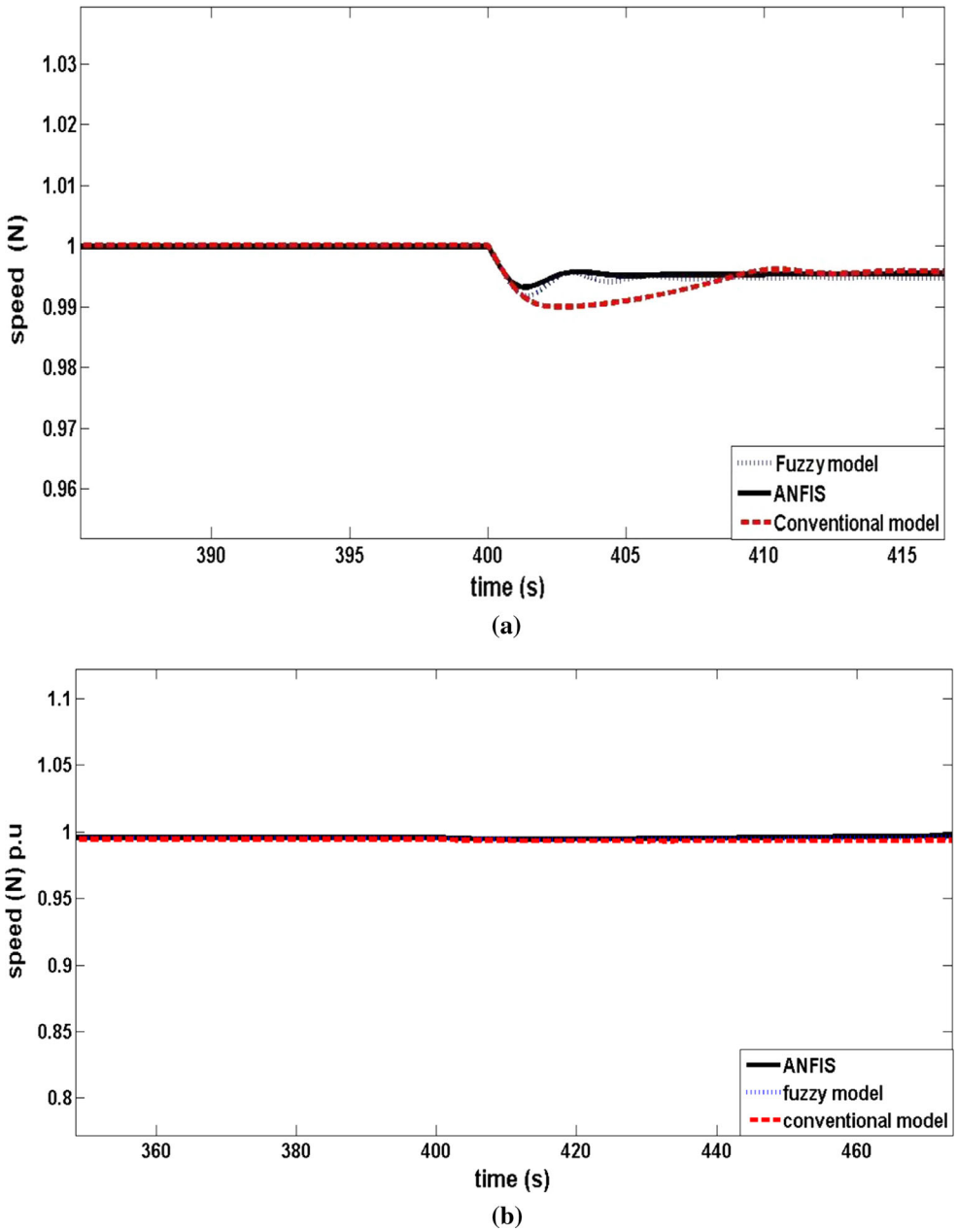

Fig. 20 Speed response of the two areas of CCGT under load perturbation operation (increasing load). **a** Speed response of area 2 of an interconnected CCGT system. **b** Speed response of area 1 of an interconnected CCGT system

Table 7 Speed response of area 2 of an interconnected ccgt system under load increase condition

Comparative coefficient	Conventional model	Fuzzy model	ANFIS
Rise time	94.1984	53.6591	51.6214
Settling time	13.9836	9.8325	4.9513
Under shoot	0.0091	0.0065	0.0056
IAE	0.0807	0.0683	0.0523
ISE	6.6057e−004	3.4416e−004	3.0132e−004
ITAE	32.6640	27.8225	21.2160

Table 8 Exhaust temperature response of area 1 of an interconnected CCGT system under load increase condition

Comparative coefficient	Conventional model	Fuzzy model	ANFIS
Rise time	8.5186	6.1223	3.7558
Settling time	66.9658	38.4539	40.9949
Over shoot	0.026	0.04	0.04

5.3 Response under load perturbation condition

Simulation studies are performed to investigate the performance of the two-area system of combined cycle gas turbine with and without the proposed fuzzy logic controllers. A step load perturbation that has amplitude 0.15 p.u is applied where the load is increased from 0.85 to 1 p.u in area 2 of the interconnected system.

Figure 20 shows the speed responses of both areas. It can be observed that the speed response of area 2 with the proposed ANFIS controller is improved compared to the fuzzy

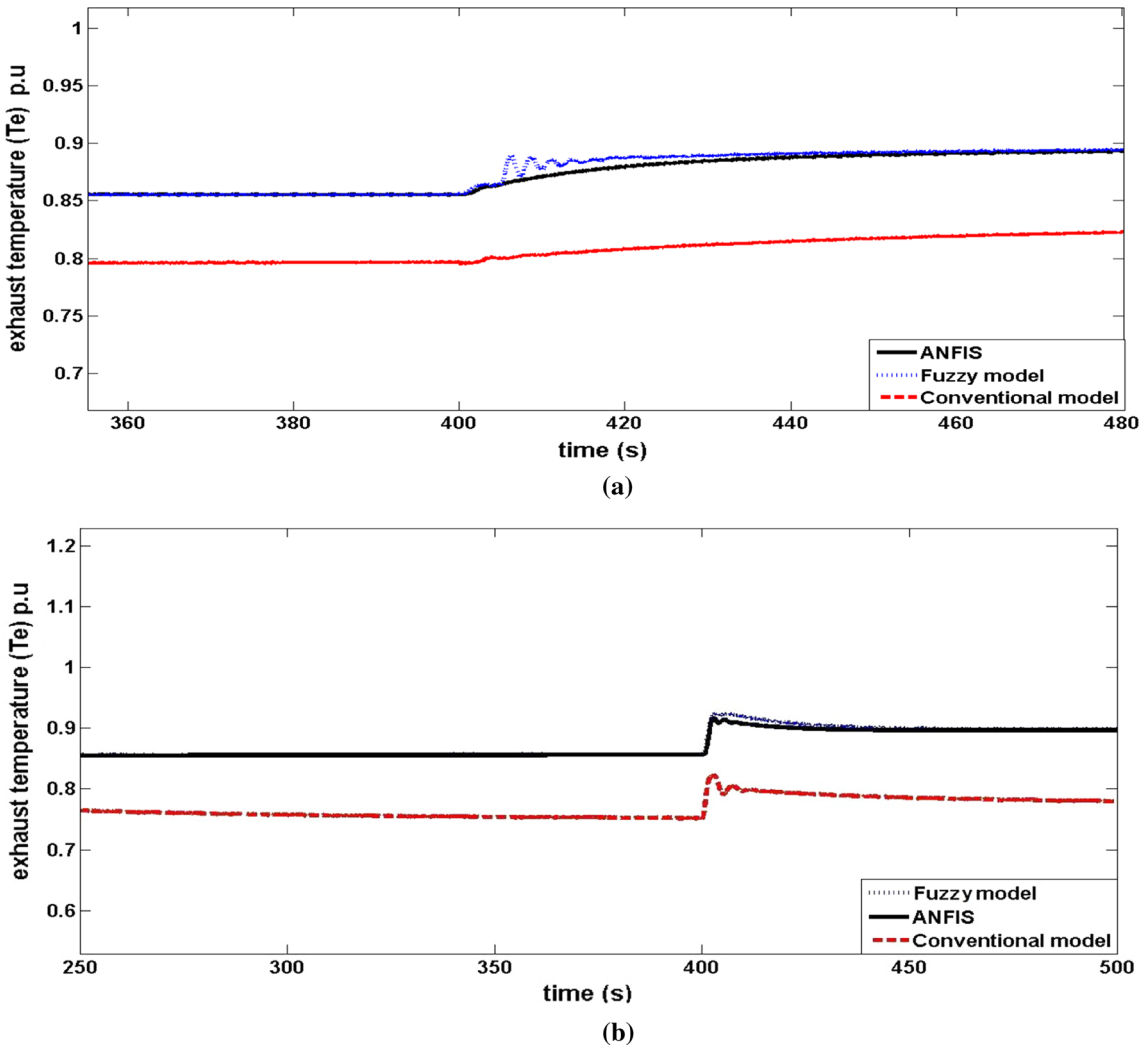

Fig. 21 Exhaust temperature (T_e) response of the two areas of CCGT under load perturbation condition (increasing load). **a** Exhaust temperature (T_e) response of area 1 of an interconnected CCGT system. **b** Exhaust temperature (T_e) response of area 2 of an interconnected CCGT system

Table 9 Exhaust temperature response of area 2 of an interconnected CCGT system under load increase condition

Comparative coefficient	Conventional model	Fuzzy model	ANFIS
Rise time	8.5186	6.1223	3.7558
Settling time	55.5611	37.4699	31.4681
Overshoot	0.025	0.0235	0.0221

Table 10 Mechanical power response of area 1 of an interconnected CCGT system under load increase condition

Comparative coefficient	Conventional model	Fuzzy model	ANFIS
Rise time	6.8508	0.6211	0.62
Settling time	53.4586	37.1504	32.6307
Overshoot	0.0749	0.0749	0.0749

logic controller and conventional controller in terms of peak deviations and settling time as shown in Table 7. The speed response of area 1 is slightly affected by this disturbance as shown in Fig. 20b. Figure 21 shows the exhaust temperature response of the two areas for a step load disturbance in area 2. The results show that the proposed ANFIS control configuration achieves better dynamic performance over the fuzzy logic and conventional controller in terms of peak deviation and settling time. In addition, the maximum exhaust temperature of the proposed ANFIS controller and fuzzy logic controller is improved compared to conventional controller and the settling time of the proposed control approach is faster than the fuzzy logic and conventional controller as shown in Tables 8 and 9.

Figure 22 shows the mechanical power (P_m) response in each area against step load disturbance. It can be seen that the

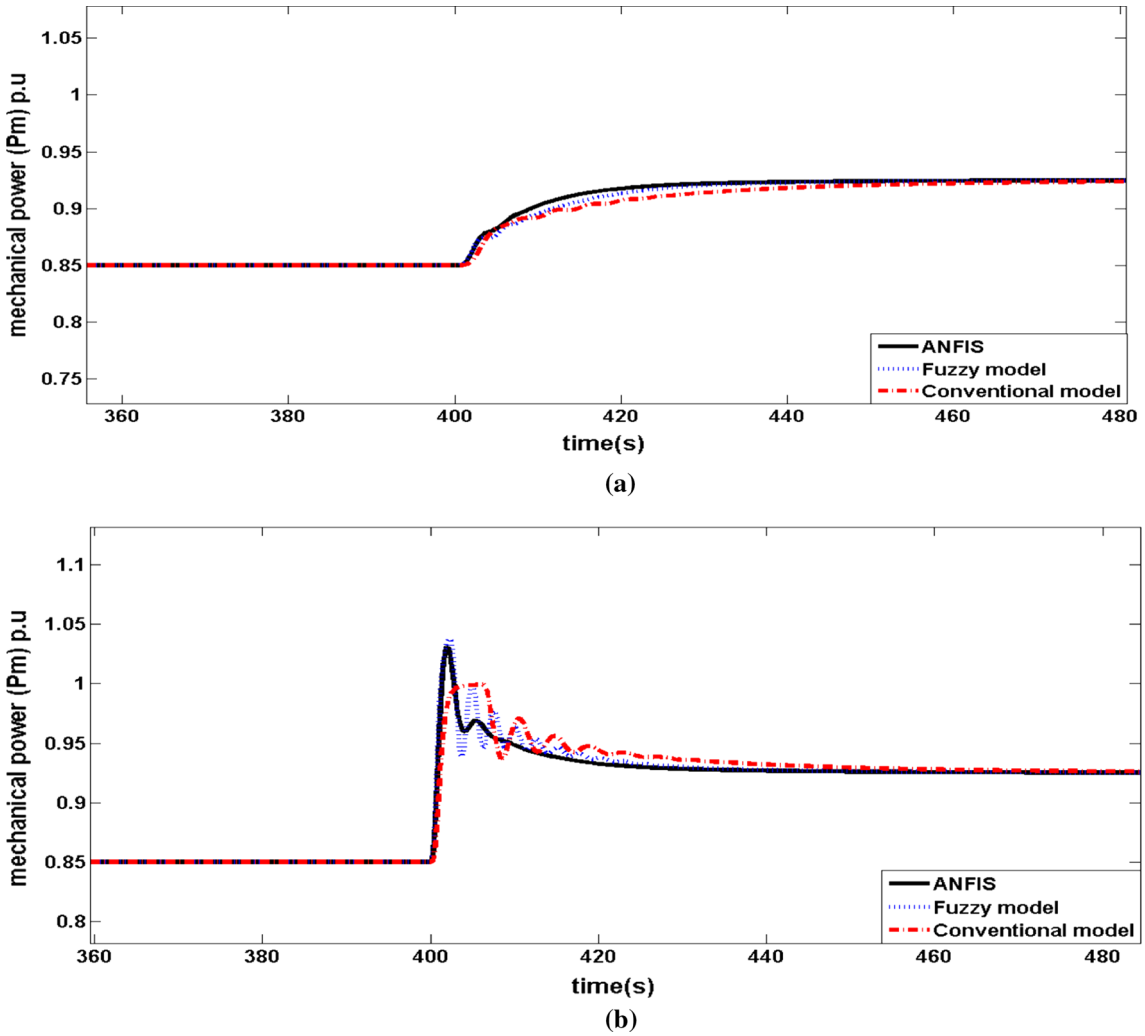

Fig. 22 Mechanical power (P_m) response of the two areas of CCGT under load perturbation operation (increasing load). **a** Mechanical power (P_m) response of area 1 of an interconnected CCGT system. **b** Mechanical power (P_m) response of area 2 of an interconnected CCGT system

Table 11 Mechanical power response of area 2 of an interconnected CCGT system under load increase condition

Comparative coefficient	Conventional model	Fuzzy model	ANFIS
Rise time	6.8508	0.6211	0.62
Settling time	56.0157	38.7171	35.7611
Overshoot	0.1493	0.1878	0.1808

ANFIS controller is much superior over the fuzzy logic and conventional controller where the transient responses of both areas are improved significantly compared to the conventional model and the proposed model with fuzzy logic controller in terms of settling time as shown in Tables 10 and 11.

To verify the robustness of the proposed control strategy, a load reduction of 0.15 p.u is applied to area 2. The results obtained show that the proposed ANFIS controllers improve effectively the damping of oscillations after a load deviation compared to the proposed fuzzy logic and conventional controllers as shown in Figs. 23, 24 and 25. Figure 23 shows the speed perturbations in each area against the load deviation in area 2. The superiority of the ANFIS controller over conventional controller and the fuzzy logic controller is quite clear where the settling time and the damping characteristics are greatly improved as shown in Table 12.

Secondly, the exhaust temperature response of the proposed ANFIS controller is improved compared to the conventional and fuzzy logic controllers as shown in Fig. 24. It is clear that the settling time and the maximum exhaust temperature are higher with the proposed ANFIS controllers as shown in Tables 13 and 14. Finally, Fig. 25 shows the mechanical power response of each area under load pertur-

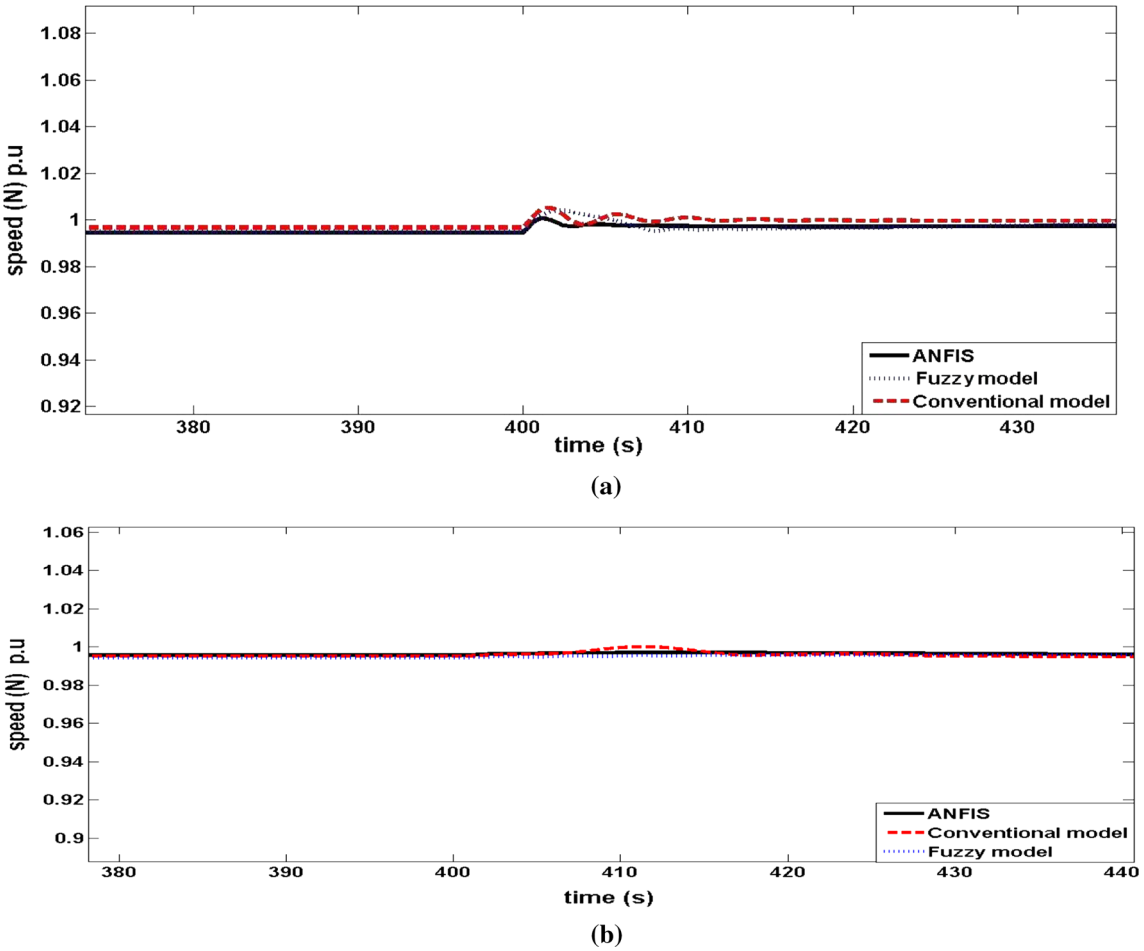

Fig. 23 Speed response of the two areas of CCGT under load perturbation operation (decreasing load). **a** Speed response of area 2 of an interconnected CCGT system. **b** Speed response of area 1 of an interconnected CCGT system

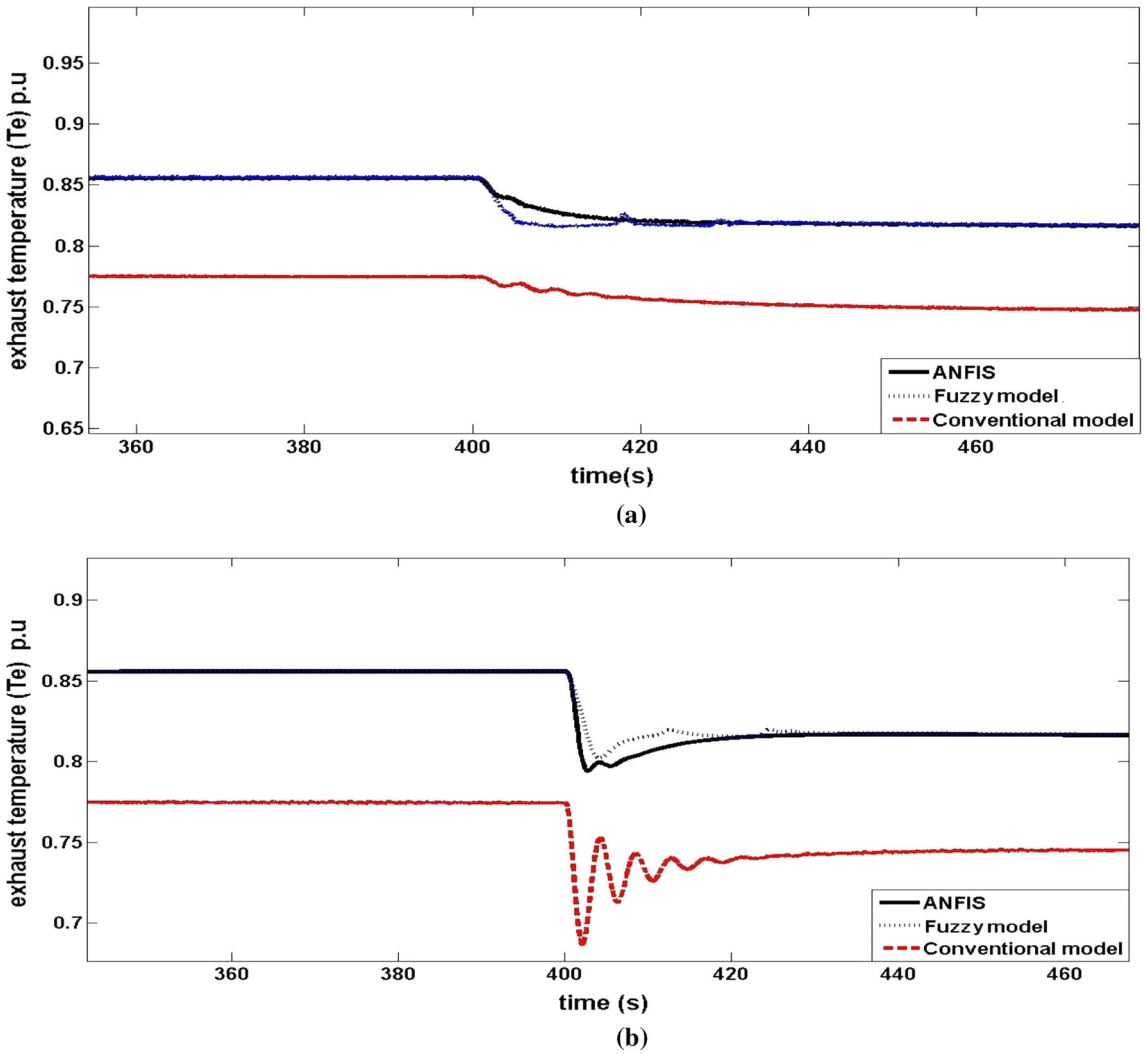

Fig. 24 Exhaust temperature (T_e) response of the two area of CCGT under load perturbation operation (decreasing load). **a** Exhaust temperature (T_e) response of area 1 of an interconnected CCGT system. **b** Exhaust temperature (T_e) response of area 2 of an interconnected CCGT system

bation in area 2. It can be concluded that the results confirm the superiority of the proposed ANFIS controllers in terms of undershoot and the settling time as shown in Tables 15 and 16.

6 Conclusion

This paper presents the model of an interconnected combined cycle gas turbine and its control loops to study the dynamic performance of CCGT and its frequency regulation. A fuzzy rule-based control is applied to design an efficient controller for both areas of the interconnect system to improve the dynamic performance of CCGT. The proposed fuzzy logic is applied to the model for both triangular membership and trapezoidal membership functions to select optimal shape of membership function. It was observed from the results that triangular membership function achieves better dynamic performance compared to trapezoidal membership function. Moreover, ANFIS controller is applied to both areas of the interconnected CCGT in order to provide an optimal operation, which gives the optimal controller parameters at any load point within the specified range. The simulation studies have been carried out under normal operating condition and after subjected to different disturbances of load variations. The results demonstrate that the proposed ANFIS controller is much more effective than the conventional and proposed fuzzy logic controller especially under load perturbation conditions.

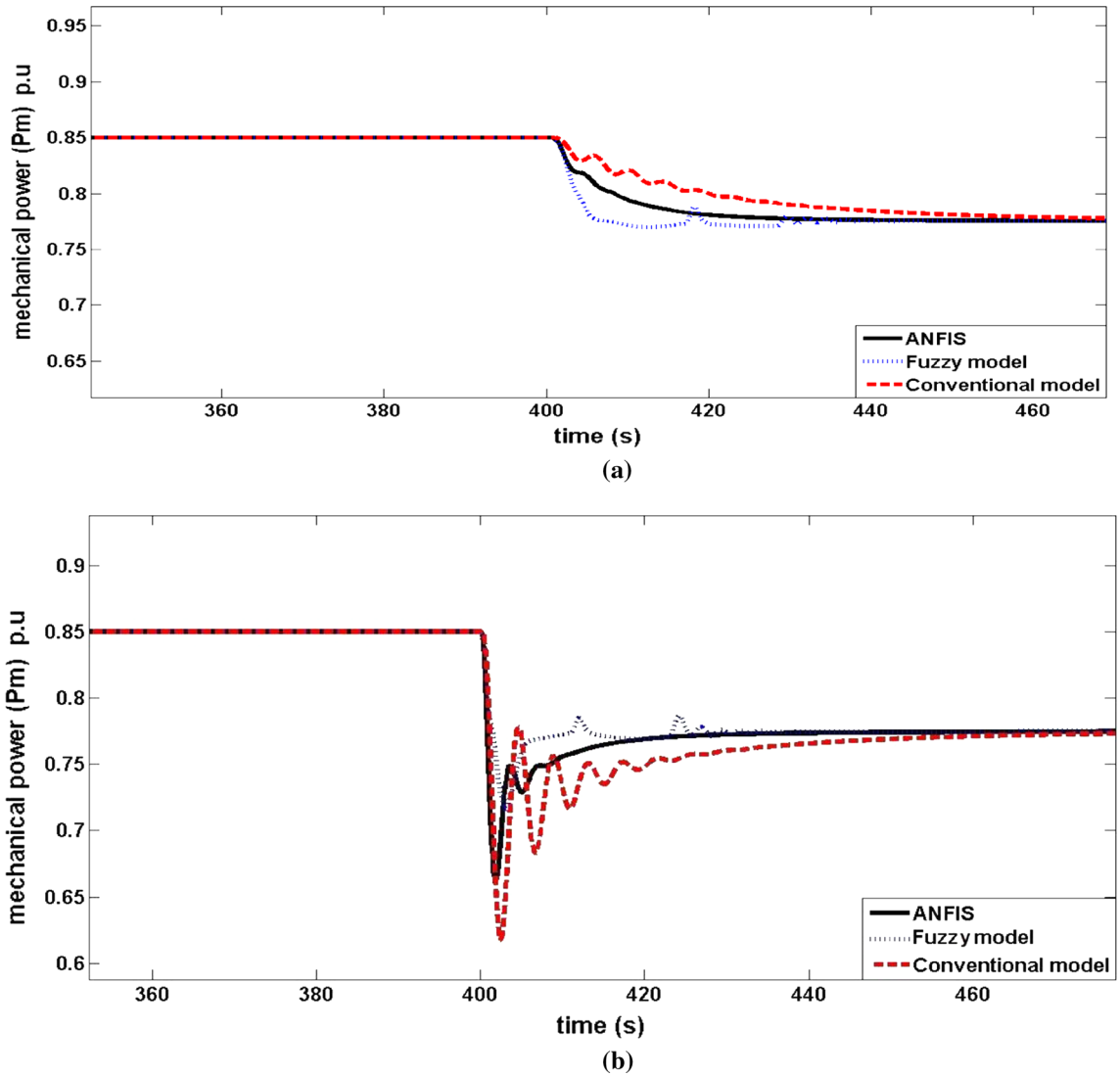

Fig. 25 Mechanical power (P_m) response of the two areas of CCGT under load perturbation operation (decreasing load). **a** Mechanical power (P_m) response of area 1 of an interconnected CCGT system. **b** Mechanical power (P_m) response of area 2 of an interconnected CCGT system

Table 12 Speed response of area 2 of an interconnected CCGT system under load decrease condition

Comparative coefficient	Conventional model	Fuzzy model	ANFIS
Rise time	94.1984	53.6591	51.6214
Settling time	16.3023	9.71	6.2424
Over shoot	0.0112	0.0109	0.0048
IAE	0.1003	0.0215	0.0097
ISE	6.5481e−004	6.6204e−005	1.8248e−005
ITAE	40.9105	8.6997	3.8989

Table 13 Exhaust temperature response of area 1 of an interconnected CCGT system under load decrease condition

Comparative coefficient	Conventional model	Fuzzy model	ANFIS
Rise time	8.5186	6.1223	3.7558
Settling time	50.751	33.5722	28.4591
Under shoot	0.014	0.0399	0.038

Table 14 Exhaust temperature response of area 2 of an interconnected CCGT system under load decrease condition

Comparative coefficient	Conventional model	Fuzzy model	ANFIS
Rise time	8.5186	6.1223	3.7558
Settling time	50.691	35.634	30.8156
Undershoot	0.0885	0.0537	0.0629

Table 15 Mechanical power response of area 1 of an interconnected CCGT system under load decrease condition

Comparative coefficient	Conventional model	Fuzzy model	ANFIS
Rise time	6.8508	0.6211	0.62
Settling time	62.4419	41.5334	36.6982
Undershoot	0.0746	0.0749	0.0749

Table 16 Mechanical power response of area 1 of an interconnected CCGT system under load decrease condition

Comparative coefficient	Conventional model	Fuzzy model	ANFIS
Rise time	6.8508	0.6211	0.62
Settling time	62.6022	35.0168	32.8622
Undershoot	0.2376	0.1342	0.1913

Acknowledgements Dr. M. A. Abido would like to acknowledge the support of King Fahd University of Petroleum and Minerals (KFUPM) through the Electrical Power and Energy Systems Research Group.

Appendix: CCGT

Table 17 shows the parameter values and the related values of CCGT model.

Table 17 CCGT parameters values

Symbol	Description	Value
$T_i^{1,2}$	Compressor inlet temperature	30 °C
$T_{\mathrm{do}}^{1,2}$	Rated compressor discharge temperature	390 °C
$T_{\mathrm{fo}}^{1,2}$	Rated gas turbine inlet temperature	1085 °C
$P_{\mathrm{ro}}^{1,2}$	Compressor pressure ratio	11.5
$\alpha^{1,2}$	Ratio of specific heat	1.4
$n_{\mathrm{c}}^{1,2}$	Compressor efficiency	0.85
$n_{\mathrm{t}}^{1,2}$	Turbine efficiency	0.85
$R^{1,2}$	Speed regulation	0.04
$T_{\mathrm{t}}^{1,2}$	Temperature control integration rate	0.469
$T_{\mathrm{cmax}}^{1,2}$	Temperature control upper limit	1.1
$T_{\mathrm{cmin}}^{1,2}$	Temperature control lower limit	0
$F_{\mathrm{dmax}}^{1,2}$	Fuel control upper limit	1.5
$F_{\mathrm{dmin}}^{1,2}$	Fuel control lower limit	0
$T_{\mathrm{v}}^{1,2}$	Valve positioner time constant	0.05
$T_{\mathrm{fu}}^{1,2}$	Fuel system time constant	0.4
$T_{\mathrm{w}}^{1,2}$	Air control time constant	0.4669
$T_{\mathrm{cd}}^{1,2}$	Compressor volume time constant	0.2
$T_{\mathrm{g}}^{1,2}$	Governor time constant	0.05
$K_0^{1,2}$	Gas turbine output coefficient	0.0033
$K_1^{1,2}$	Steam turbine output coefficient	0.00043
$T_{\mathrm{m}}^{1,2}$	Tube metal heat capacitance time constant of waste heat recovery boiler	5
$T_{\mathrm{b}}^{1,2}$	Boiler storage time constant of waste heat recovery boiler	20
$T_{\mathrm{I}}^{1,2}$	Turbine rotor time constant	18.5
$K_3^{1,2}$	Ratio of fuel adjustment	0.77
$K_4^{1,2}$	Gain of radiation shield	0.8
$K_5^{1,2}$	Gain of radiation shield	0.2
$K_6^{1,2}$	Fuel valve lower limit	0.23
$T_3^{1,2}$	Radiation shield time constant	15
$T_4^{1,2}$	Thermocouple time constant	2.5
$T_5^{1,2}$	Temperature control time constant	3.3
T_{12}	Synchronizing power coefficient	0.545
$K_{\mathrm{c}}^{1,2}$	Speed control integral gain	

References

1. Finn J, Wagner J, Bassily H (2010) Monitoring strategies for a combined cycle electric power generator. Appl Energy 87(8):2621–2627
2. Demirören A (2002) Application of a self-tuning to automatic generation control in power system including SMES units. Eur Trans Electr Power 12(2):101–109
3. Abraham RJ, Das D, Patra A (2007) Automatic generation control of an interconnected hydrothermal power system considering superconducting magnetic energy storage. Int J Electr Power Energy Syst 29(8):571–579
4. Saikia LC et al (2011) Automatic generation control of a multi area hydrothermal system using reinforced learning neural network controller. Int J Electr Power Energy Syst 33(4):1101–1108
5. Alomoush MI (2010) Load frequency control and automatic generation control using fractional-order controllers. Electr Eng 91(7):357–368
6. Demirören A, Kent S, Günel T (2002) A genetic approach to the optimization of automatic generation control parameters for power systems. Eur Trans Electr Power 12(4):275–281
7. Golpira H, Bevrani H (2011) Application of GA optimization for automatic generation control design in an interconnected power system. Energy Convers Manag 52(5):2247–2255
8. Ghoshal SP (2004) Application of GA/GA-SA based fuzzy automatic generation control of a multi-area thermal generating system. Electr Power Syst Res 70(2):115–127
9. Bhatt P, Roy R, Ghoshal SP (2010) GA/particle swarm intelligence based optimization of two specific varieties of controller devices applied to two-area multi-units automatic generation control. Int J Electr Power Energy Syst 32(4):299–310
10. Gozde H, Taplamacioglu MC (2011) Automatic generation control application with craziness based particle swarm optimization in a thermal power system. Int J Electr Power Energy Syst 33(1): 8–16
11. Ghoshal SP (2004) Optimizations of PID gains by particle swarm optimizations in fuzzy based automatic generation control. Electr Power Syst Res 72(3):203–212
12. Khodabakhshian A, Hooshmand R (2010) A new PID controller design for automatic generation control of hydro power systems. Int J Electr Power Energy Syst 32(5):375–382
13. Nikpey H, Assadi M, Breuhaus P (2013) Development of an optimized artificial neural network model for combined heat and power micro gas turbines. Appl Energy 108:137–148
14. Kalogirou SA (2000) Applications of artificial neural-networks for energy systems. Appl Energy 67(1):17–35
15. Zeynelgil HL, Demiroren A, Sengor NS (2002) The application of ANN technique to automatic generation control for multi-area power system. Int J Electr Power Energy Syst 24(5):345 –354
16. Demirören A, Zeynelgil HL, Sengör NS (2003) The application of NN technique to automatic generation control for the power system with three areas including SMES units. Eur Trans Electr Power 13(4):227–238
17. Bhongade S, Gupta HO, Tyagi B (2010) Artificial neural network based automatic generation control scheme for deregulated electricity market. In: IPEC, 2010 conference proceedings. IEEE
18. Khuntia SR, Panda S (2012) Simulation study for automatic generation control of a multi-area power system by ANFIS approach. Appl Soft Comput 12(1):333–341
19. Kumar TB, Vani M (2014) Load frequency control in two area power system using ANFIS. IISTE 5:27–35
20. Subbaraj P, Manickavasagam K (2008) Automatic generation control of multi-area power system using fuzzy logic controller. Eur Trans Electr Power 18(3):266–280
21. Demiroren A, Yesil E (2004) Automatic generation control with fuzzy logic controllers in the power system including SMES units. Electr Power Energy Syst 26:291–305
22. Mazhabjafari M, Jafari Ali M, Saidabadi K (2011) Notice of retraction modeling and simulation of combined cycle power plants participating in network frequency control. In: Power engineering and automation conference (PEAM), 2011 IEEE. IEEE, pp 112–115
23. Iliescu Sergiu ST et al (2008) Gas turbine modeling for load-frequency control. In: Scientific Bulletin, University POLITEHNICA Bucharest. Ser C Electr Eng 70:4
24. Zhang Q, SO PL (2000) Dynamic modeling of a combined cycle plant for power system stability studies. In: Power engineering society winter meeting, 2000. IEEE. IEEE, pp 1538–1543
25. Tică A, Guéguen H, Dumur D, Faille D, Davelaar F (2012) Design of a combined cycle power plant model for optimization. Appl Energy 98:256–265
26. Sasaki T, Enomoto K (2002) Dynamic analysis of generation control performance standards. IEEE Trans Power Syst 17:806–811
27. Baba K, Kakimoto N (2003) Dynamic behavior of a combined cycle power plant in the presence of a frequency drop. Electr Eng Jpn 143:9–19
28. Ning CN, Lu CN (2006) Effects of temperature control on combined cycle unit output response. In: TENCON 2006. 2006 IEEE region 10 conference. IEEE, pp 1–4
29. Kalantar M (2010) Dynamic behavior of a stand-alone hybrid power generation system of wind turbine, microturbine, solar array and battery storage. Appl Energy 87(10):3051–3064
30. Saikia LC, Sahu SK (2013) Automatic generation control of a combined cycle gas turbine plant with classical controllers using firefly algorithm. Int J Electr Power Energy Syst 53:27–33
31. Weimin K et al (2011) Study on the mathematical model and primary frequency regulation characteristics of combined cycle plants. In: 2011 second international conference on mechanic automation and control engineering (MACE). IEEE, pp 2632–2635
32. Gao L, Xia J, Dai Y (2010) Modeling of combined cycle power plant based on a genetic algorithm parameter identification method. In: 2010 sixth international conference on natural computation (ICNC). IEEE, pp 3369–3373
33. Najimi I, Ramezani MH (2012) Robust control of speed and temperature in a power plant gas turbine. ISA Trans 51(2):304–308
34. Obara S (2015) Dynamic-characteristics analysis of an independent microgrid consisting of a SOFC triple combined cycle power generation system and large-scale photovoltaics. Appl Energy 141:19–31
35. Sánchez-Parra M, De-Lara-Jayme S, Bahamaca-Fernández LJ (2002) A fuzzy-logic rule based speed and load controller for combustion turbines in power generation. In: American control conference, 2002. Proceedings of the 2002. IEEE. pp 2659–2664
36. Aboel-ela M, Fetoh A, Gamal AB (2011) Fuzzy speed controllers of combined cycle power plants. Int J Innov Electr Power Syst 3(2):109–121
37. Sanchez-Parra M et al (2012) Intelligent coordinated control for combined cycle power plants. In: 2012 IEEE international conference on control applications (CCA). IEEE, pp 148–153
38. Hosseini SH, Etemadi AH (2008) Adaptive neuro-fuzzy inference system based automatic generation control. Electr Power Syst Res 78(7):1230–1239
39. Rowen WI (1983) Simplified mathematical representations of heavy-duty gas turbines. J Eng Gas Turbines Power 105(4):865–869
40. Rowen WI (1992) Simplified mathematical representations of single shaft gas turbines in mechanical drive service. Turbomach Int 33:5
41. Shalan HEMA, Hassan MA, Moustafa Bahgat ABG (Dec. 2010) Comparative study on modeling of gas turbines in combined cycle power plants. In: Proceedings of the 14th international middle

east power systems conference (MEPCON'10), Cairo University, Egypt, pp 970–976
42. Kunitomi K et al (2001) Modeling frequency dependency of gas turbine output. In: Power engineering society winter meeting, 2001. IEEE. IEEE, pp 678–683
43. De Mello FP et al (1994) Dynamics models for combines cycle plants in power system studies. IEEE Trans Power Syst 9(3):1698–1708
44. Hannett LN, Khan A (1993) Combustion turbine dynamic model validation from tests. IEEE Trans Power Syst 8(1):152–158
45. Kakimoto N, Baba K (2003) Performance of gas turbine-based plants during frequency drops. IEEE Trans Power Syst 18(3):1110–1115
46. Rai JN et al (2013) Performance analysis of CCGT power plant using MATLAB/Simulink based simulation. Int J Adv Technol 2:285–290
47. Amgad H Salah, Mostafa A Elhosseini, Ragab A El Sehiemy, Kamal M Shebl (2015) Fuzzy-based modeling and control of combined cycle gas turbine plants. In: 17th international middle east power systems conference, December 15–17
48. Raduca M et al (2011) Fuzzy controller for adjustment of liquid level in the tank. Ann Univ Craiova Math Comput Sci Ser 38(4):33–43